Figures for Public Review

PREFACE

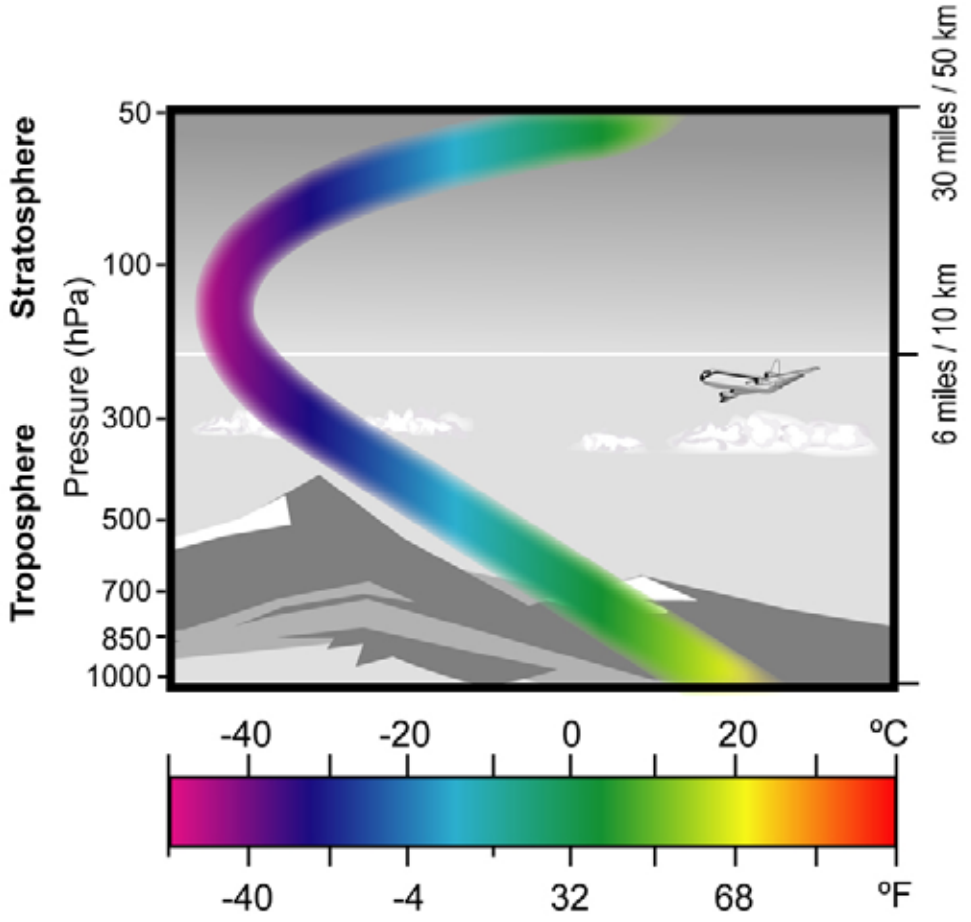

Preface Figure 1

This illustration shows the layers of the atmosphere of primary interest to this Synthesis/Assessment Report. The multi-colored line on this diagram indicates the variations in temperature with altitude.

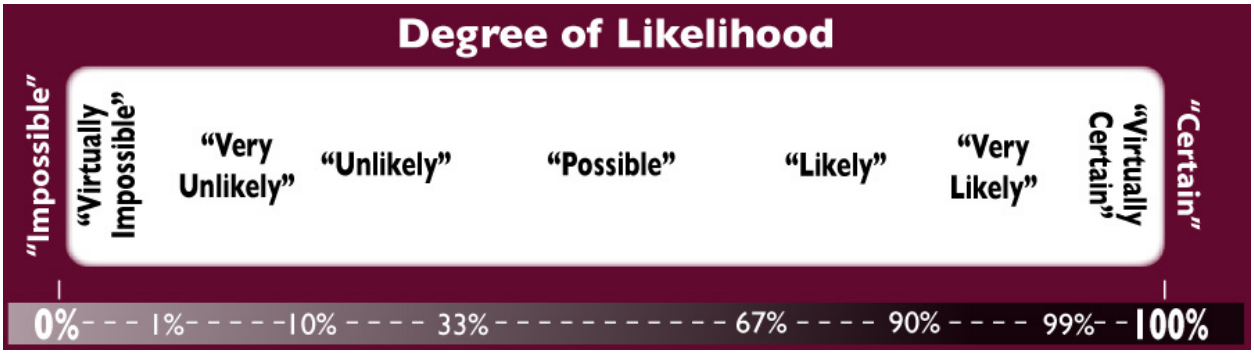

Preface Figure 2

To integrate a wide variety of information, this Report also uses a lexicon of terms to express the team's considered judgment about the likelihood of results. Confidence in results is highest at each end of the spectrum. Unless otherwise noted, all statements are certain.

EXECUTIVE SUMMARY

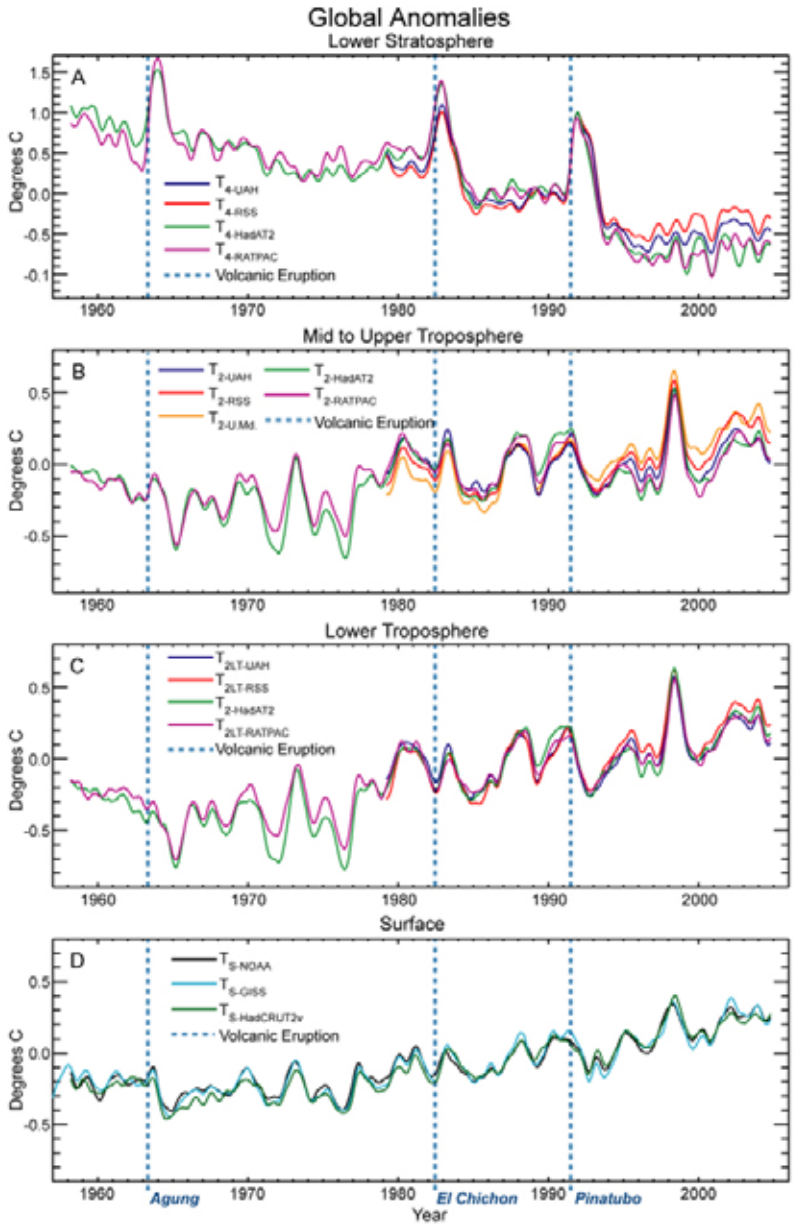

Executive Summary Figure 1: Observed surface and upper air global-mean temperature records. From top to bottom: A, lower stratosphere (denoted T_4) records from two satellite analyses (UAH and RSS) together with equivalently-weighted radiosonde records based on HadAT2 and RATPAC data; B, mid- to upper-troposphere (T_2) records from three satellite analyses (UAH, RSS and U.Md.) together with equivalently-weighted radiosonde records based on HadAT2 and RATPAC; C, lower troposphere (T_{2LT}) records from UAH and RSS (satellite), and from HadAT2 and RATPAC (equivalently-weighted radiosonde); D, surface (T_S). All time series are based on monthly-mean data smoothed with a 7-month running average, expressed as departures from the Jan. 1979 to Dec. 1997 average. Note that the T_2 data (panel B) contain a small contribution (about 10%) from the lower stratosphere. Information here is from Figures 3.1, 3.2 and 3.3 in Chapter 3.

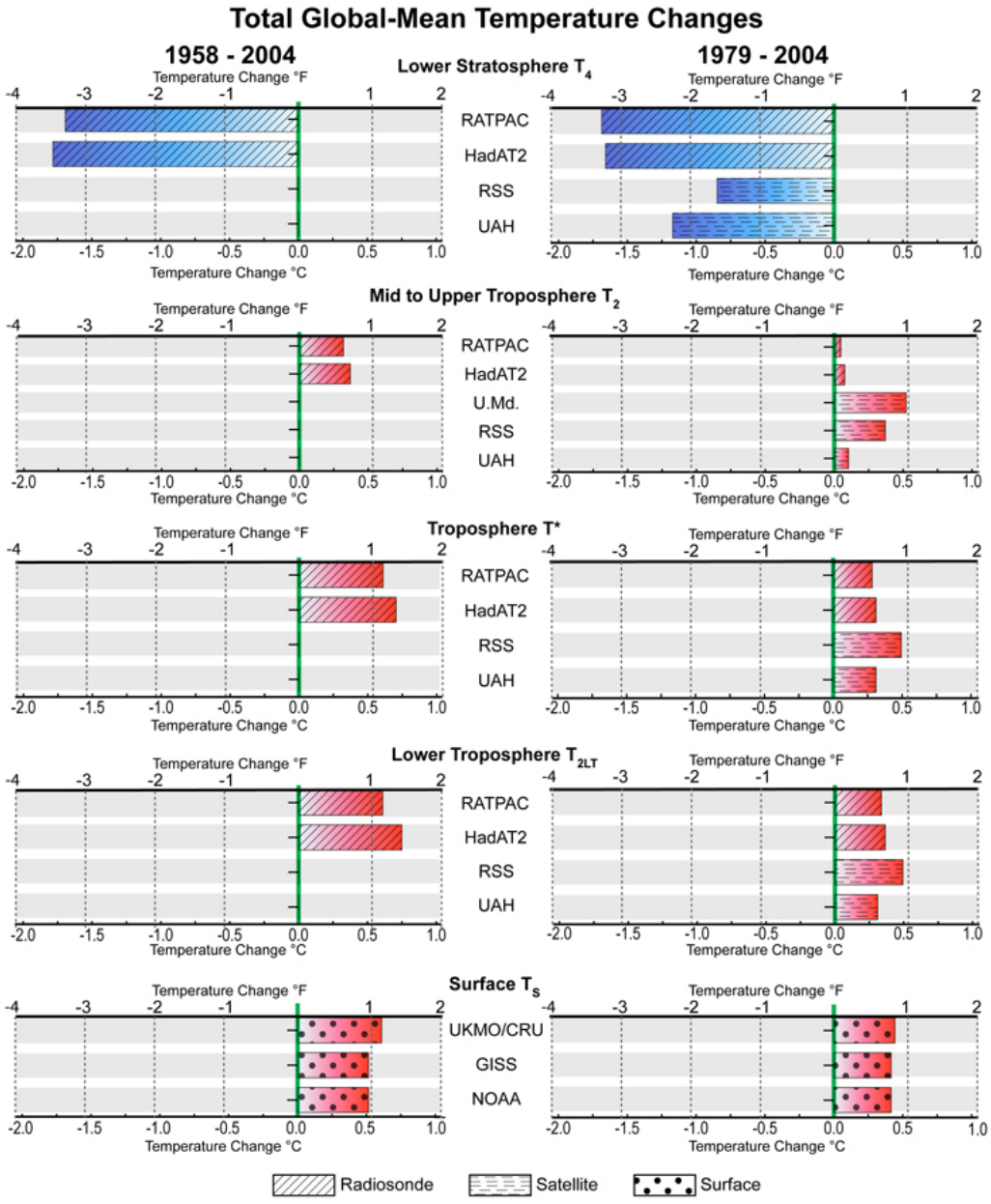

Executive Summary Figure 2: Total global-mean temperature changes for the surface and different atmospheric layers, from different data sets and over two periods, 1958 to 2004 and 1979 to 2004. The values shown are the total change over the stated period in both degrees Celsius (degC; lower scales) and degrees Fahrenheit (degF; upper scales). All changes are statistically significant at the 5% level except RSS T_4 and RATPAC, HadAT2 and UAH T_2. Total change in degC is the linear trend in degC per decade (see Tables 3.2 and 3.3 in Chapter 3) times the number of decades in the time period considered. Total change in degF is this number times 1.8 to convert to degF. For example, the Table 3.2 trend for NOAA surface temperatures over January 1958 through December 2004 is 0.11°C/decade. The total change is therefore 0.11 times 4.7 decades to give a total change of 0.53°C, Multiplying this by 1.8 gives a total change in degrees Fahrenheit of 0.93°F. Warming is shown in red, and cooling in blue.

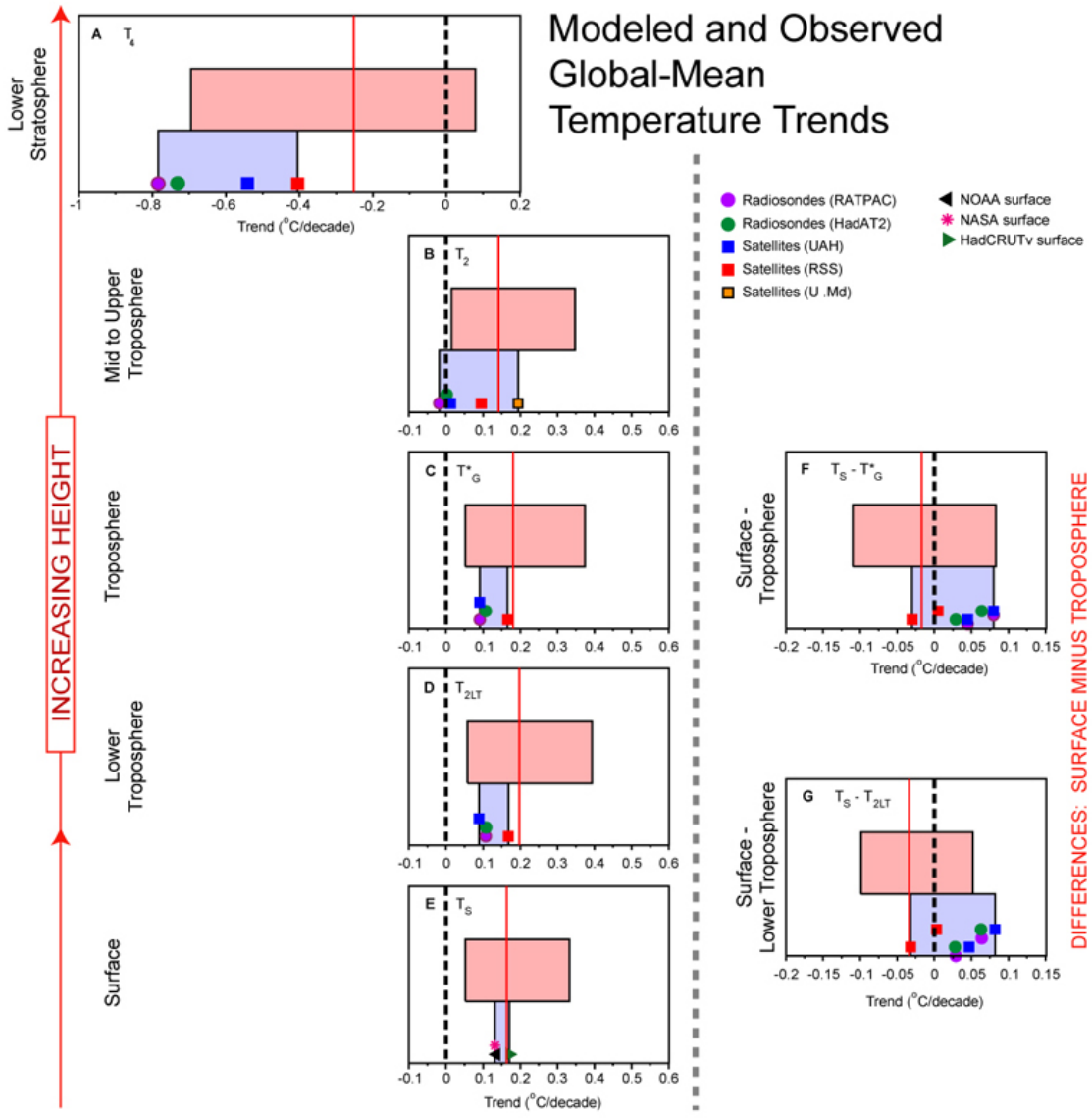

Executive Summary Figure 3: Comparison of observed and model-simulated global-mean temperature trends (left-hand panels) and trend differences (right-hand panels) over January 1979 through December 1999, based on Table 5.4A and Figure 5.3 in Chapter 5. The upper red rectangles in each box show the range of model trends from 49 model simulations. The lower blue rectangles show the range of observed trends, with the individual trends from different data sets indicated by the symbols. From bottom to top, the left-hand panels show trends for the surface (T_S), the lower troposphere (T_{2LT}), the troposphere (T^*), the mid troposphere to lower stratosphere (T_2), and the lower stratosphere (T_4). The right-hand panels show differences in trends between the surface and either the troposphere or the lower troposphere, with a positive value indicating a stronger warming at the surface. The red vertical lines show the average of all model results. The vertical black dashed lines show the zero value. For the observed trend differences, there are eight values corresponding to combinations of the four upper-air data sets (as indicated by the symbols) and either the HadCRUT2v surface data or the NASA/NOAA surface data (which have almost identical trends).

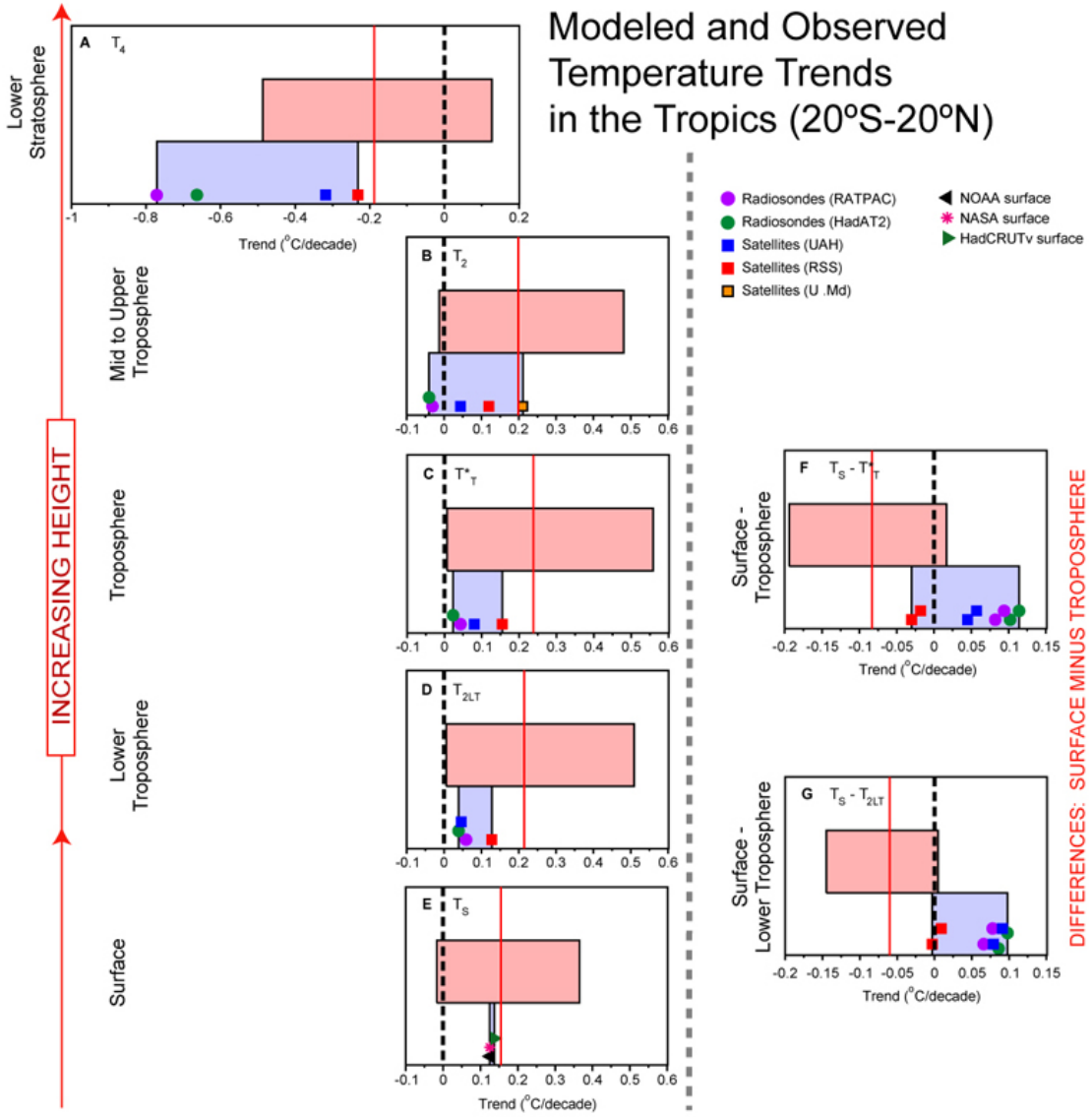

Executive Summary Figure 4: As Figure 3, but for the tropics (20ºS to 20ºN), based on Table 5.4B and Figure 5.4 in Chapter 5.

CHAPTER 1

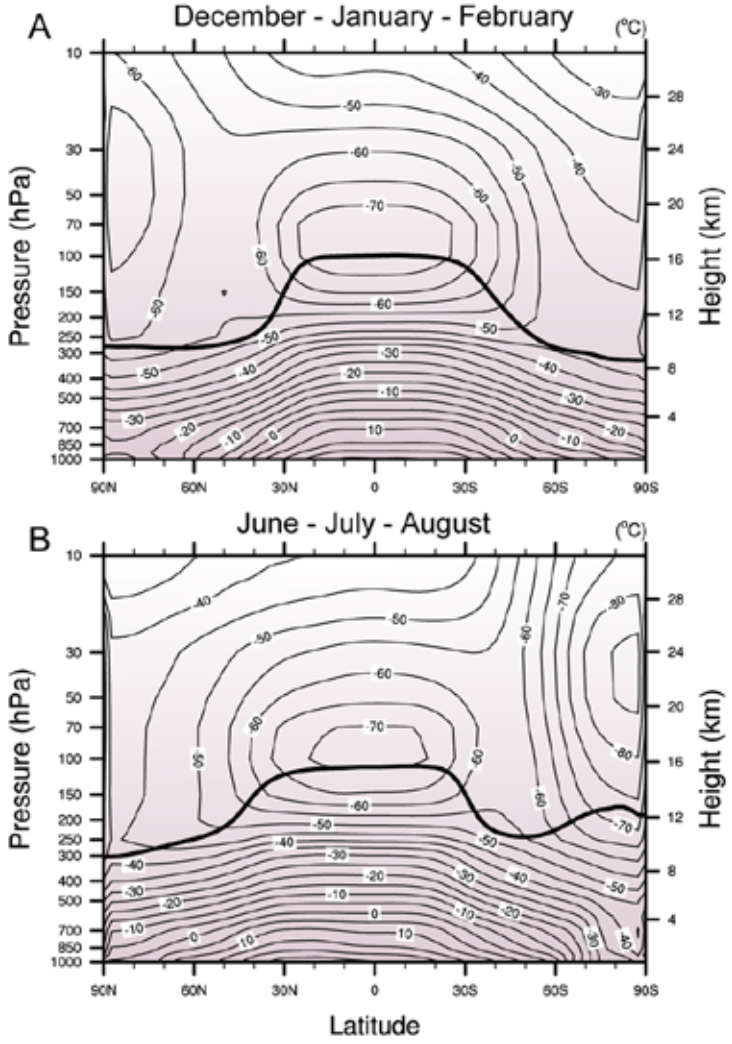

Figure 1.1. Global climatological vertical temperature profiles from surface to troposphere and extending into the stratosphere for December-January-February and June-July-August mean conditions, as obtained from the National Centers for Environmental Prediction reanalyses (Kalnay et al., 1996; updated). The solid line denotes the tropopause which separates the stratosphere from the surface-troposphere system.

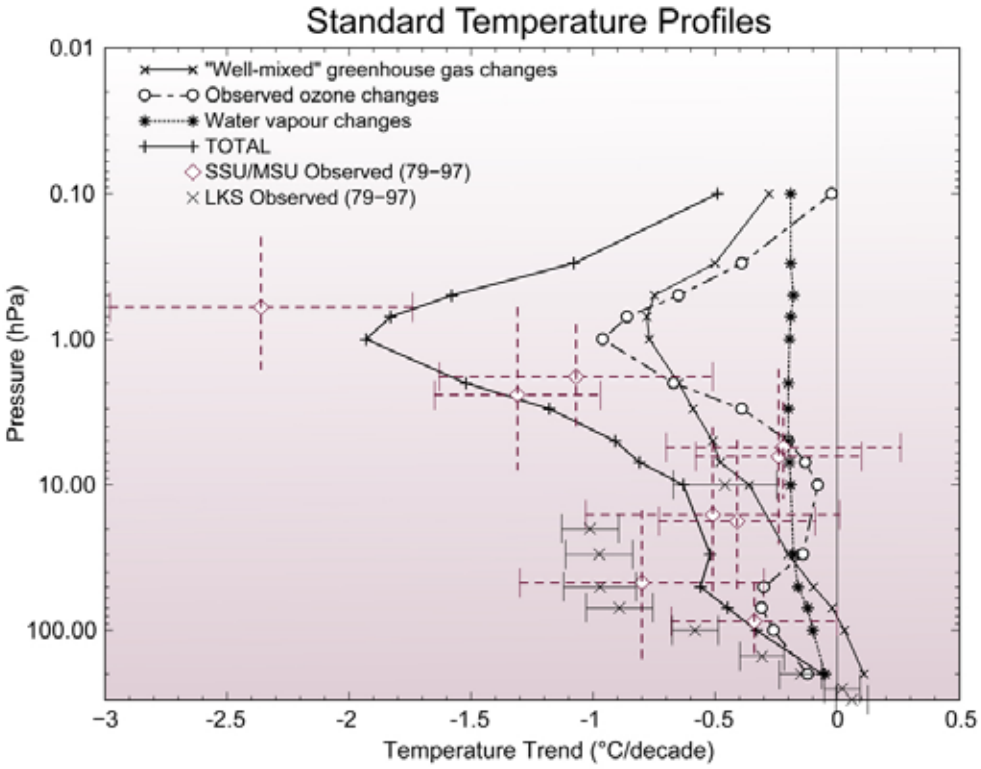

Figure 1.2. Global- and annual-mean temperature change over the 1979-1997 period in the stratosphere. Observations: LKS (radiosonde), SSU and MSU (satellite) data.
Vertical bars on satellite data indicate the approximate span in altitude from where the signals originate, while the horizontal bars are a measure of the uncertainty in the trend. Computed: effects due to increases in well-mixed gases, water vapor, and ozone depletion, and the total effect (Shine et al., 2003).

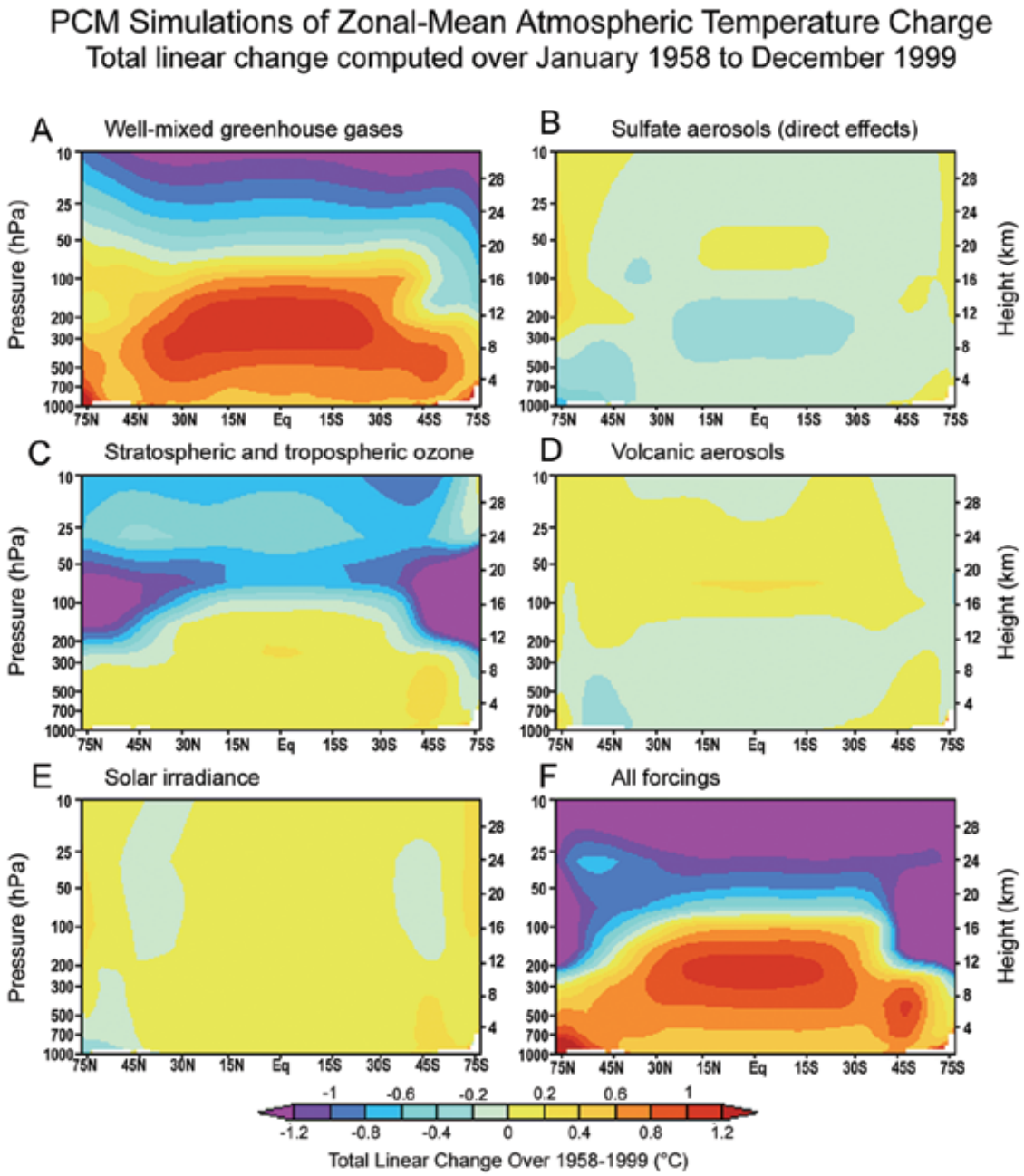

Figure 1.3. PCM simulations of the vertical profile of temperature change due to various forcings, and the effect due to all forcings taken together (after Santer et al., 2000).

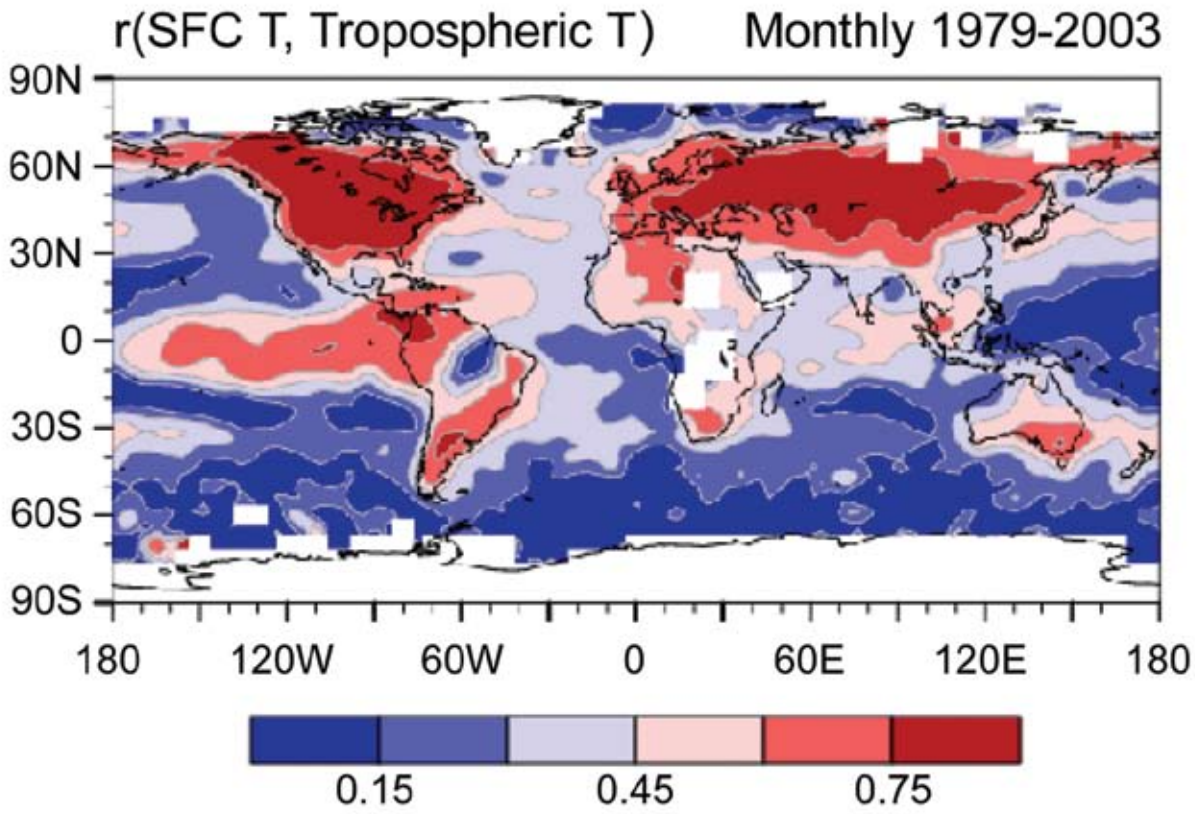

Figure 1.4. Gridpoint correlation coefficients between monthly surface and tropospheric temperature anomalies over 1979-2003. The tropospheric temperatures are derived from MSU satellite data (Christy et al., 2003).

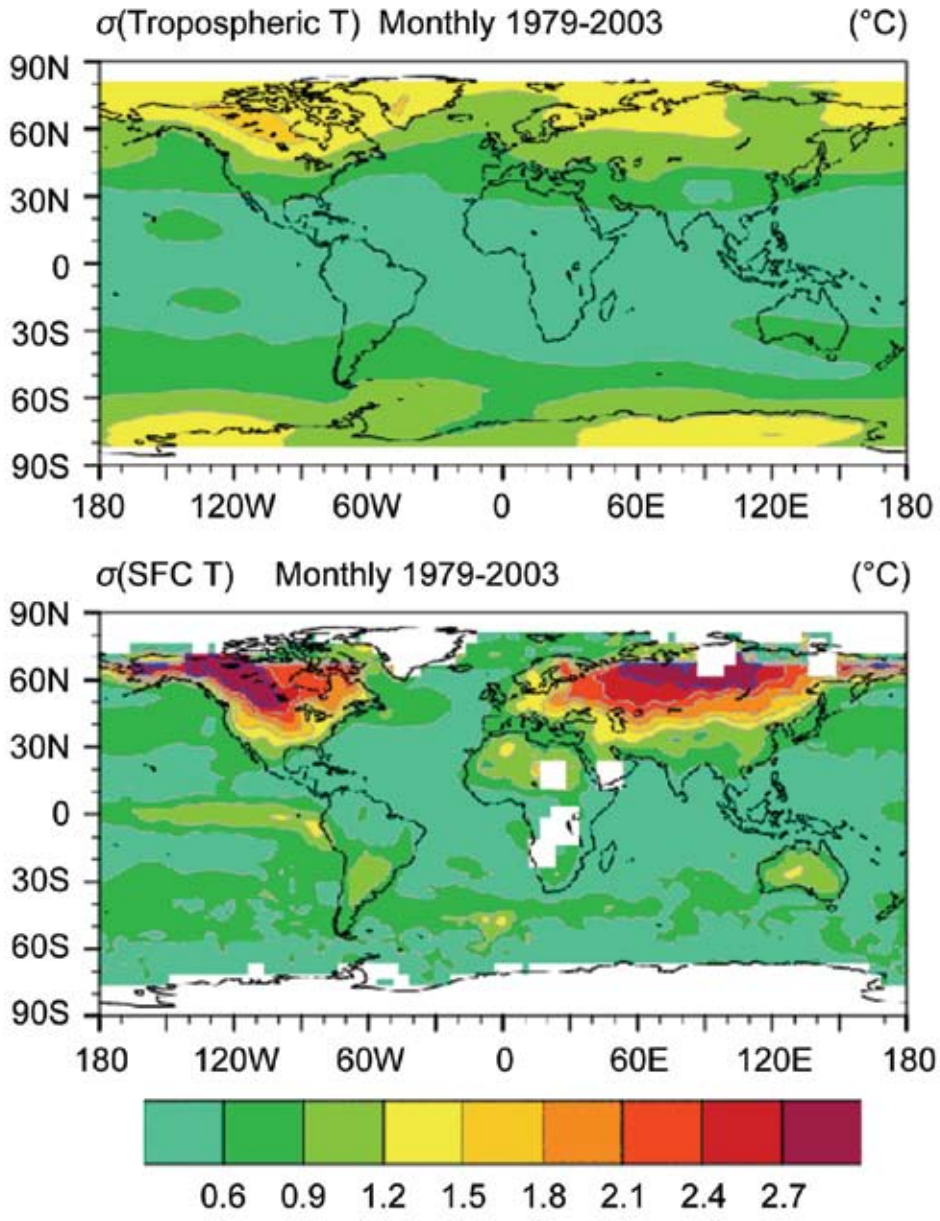

Figure 1.5. Standard deviations of monthly mean temperature anomalies from the surface and tropospheric temperature records over 1979-2003. The tropospheric temperatures are derived from MSU satellite data (Christy et al., 2003).

CHAPTER 2

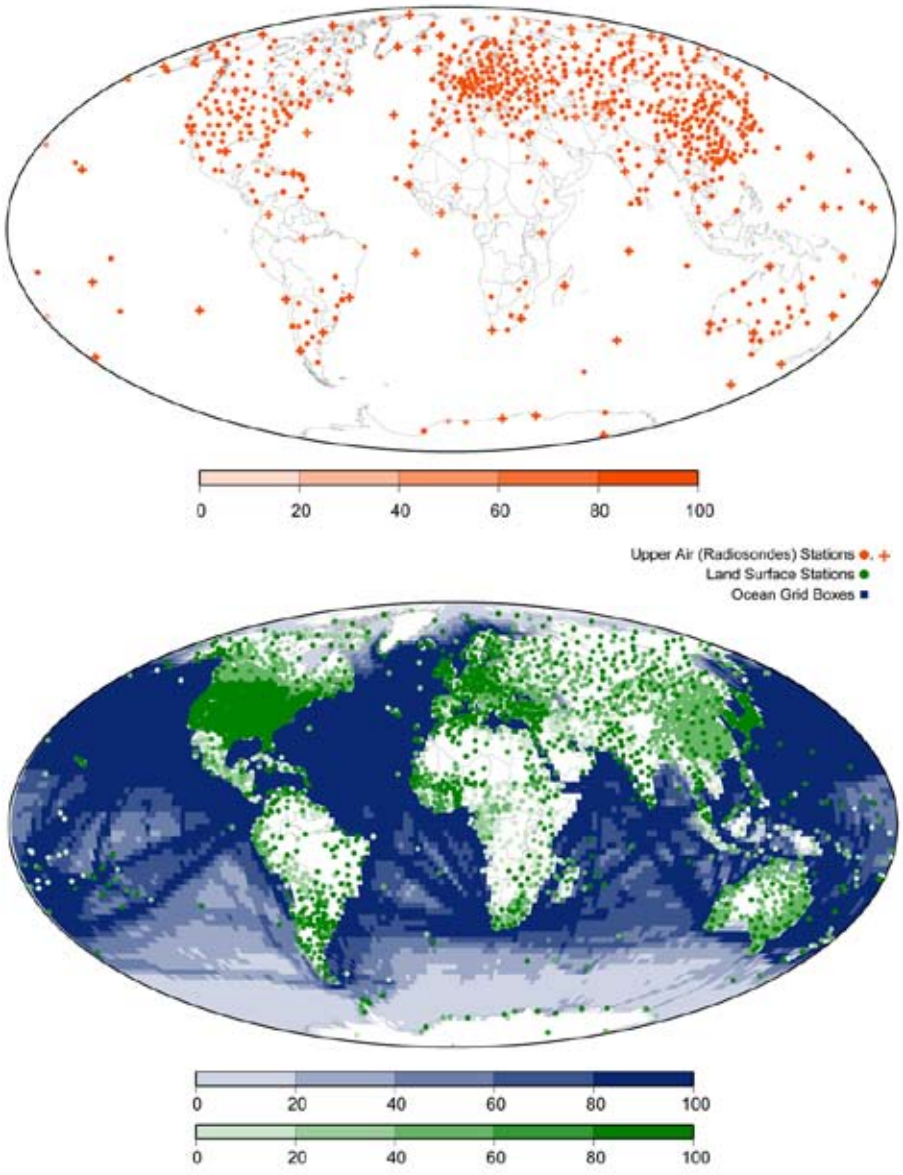

Figure 2.1 Top: Location of radiosonde stations used in the HadAT upper air dataset with those also in the LKS as crosses. Bottom: Distribution of land stations (green) and SST observations (blue) reporting temperatures used in the surface temperature datasets over the period 1979-2004. Darker colors represent locations for which data were reported with greater frequency. See chapter 3 for definitions of datasets.

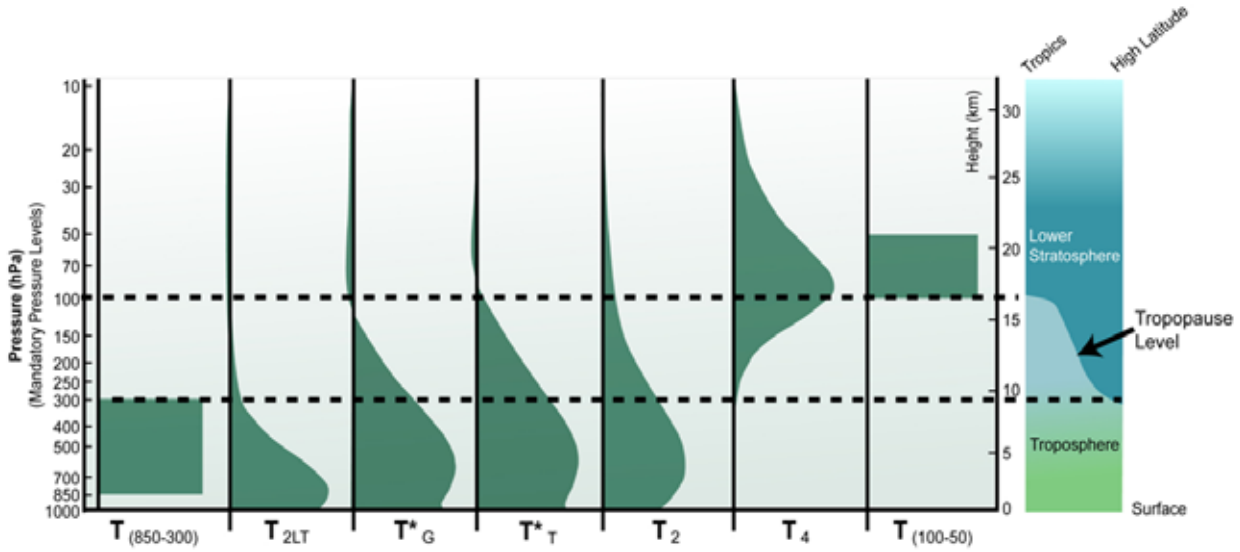

Figure 2.2 Terminology and vertical profiles for the temperature products referred to in this report. Radiosonde-based layer temperatures ($T_{850-300}$, T_{100-50}) are height-weighted averages of the temperature in those layers. Satellite-based temperatures (T_{2LT}, T_2, and T_4) are mass-weighted averages with varying influence in the vertical as depicted by the curved profiles, i.e., the larger the value at a specific level, the more that level contributes to the overall satellite temperature average. The subscript simply indicates the layer where 90% of the information for the satellite average originates.

Notes: (1) because radiosondes measure the temperature at discrete (mandatory) levels, their information may be used to create a temperature value that mimics a satellite temperature (Text Box 2.1), (2) layer temperatures vary from equator to pole so the pressure and altitude relationship here is based on the atmospheric structure over the conterminous U.S., (3) about 10% (5%) of the value of T_{2LT} (T_2) is determined by the surface character and temperature, (4) T^*_T and T^*_G are simple retrievals, being linear combinations of 2 channels, T_2 and T_4.

CHAPTER 3

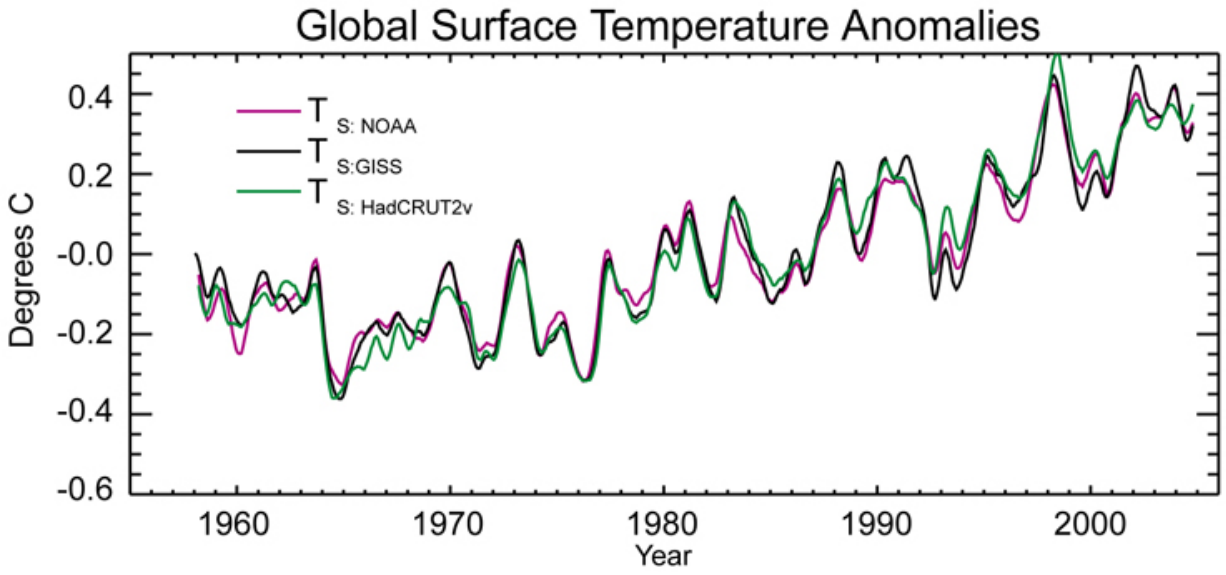

Figure 3.1 - Time series of globally averaged surface temperature (T_S) for NOAA (violet), GISS (black), and HadCRUT2v (green) datasets. All time series are 7-month running averages (used as a smoother) of original monthly data, which were expressed as a departure (ºC) from the 1979-97 average.

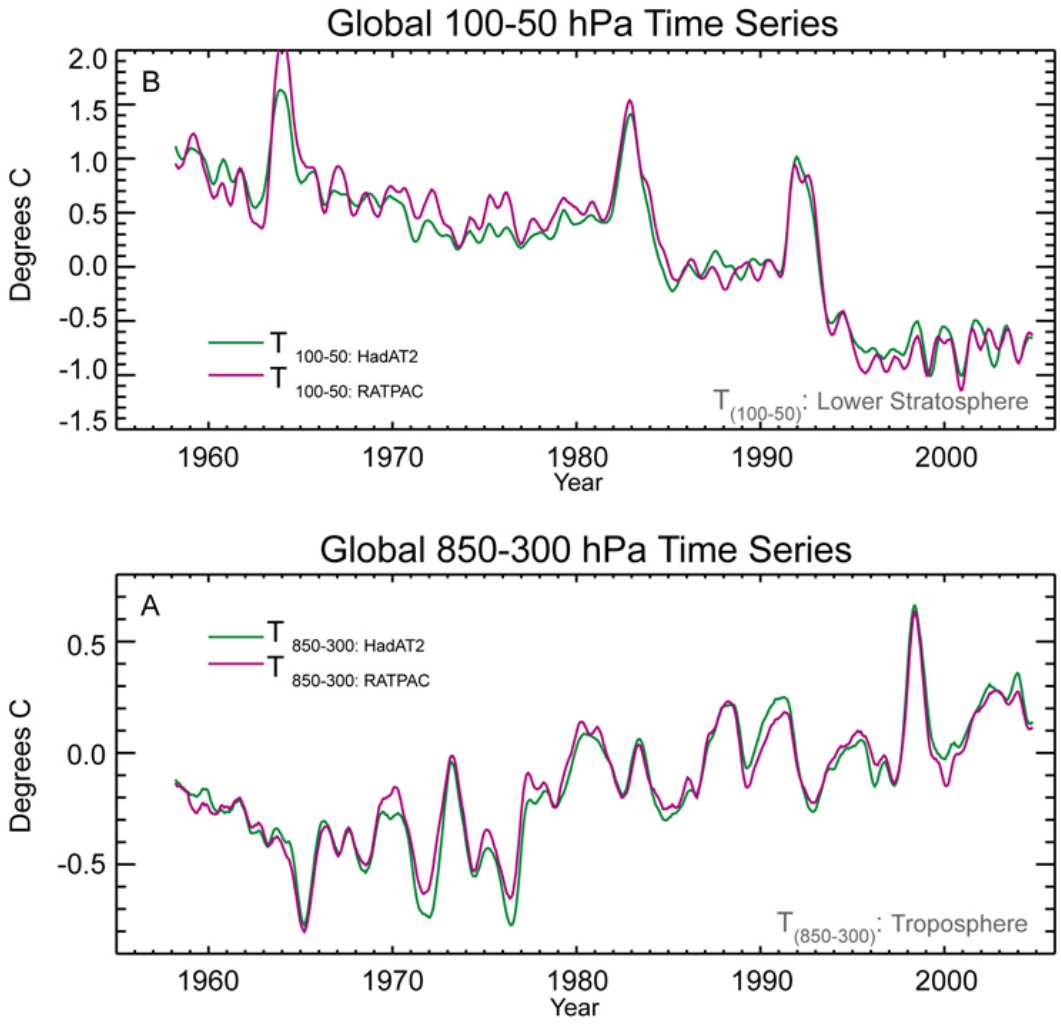

Figure 3.2a – Bottom: Time series of globally averaged tropospheric temperature ($T_{(850-300)}$) for RATPAC (violet) and HadAT2 (green) radiosonde datasets. All time series are 7-month running averages (used as a smoother) of original monthly data, which were expressed as a departure (ºC) from the 1979-97 average.

Figure 3.2b – Top: Time series of globally averaged stratospheric temperature ($T_{(100-50)}$) for RATPAC (violet) and HadAT2 (green) radiosonde datasets. All time series are 7-month running averages (used as a smoother) of original monthly data, which were expressed as a departure (ºC) from the 1979-97 average.

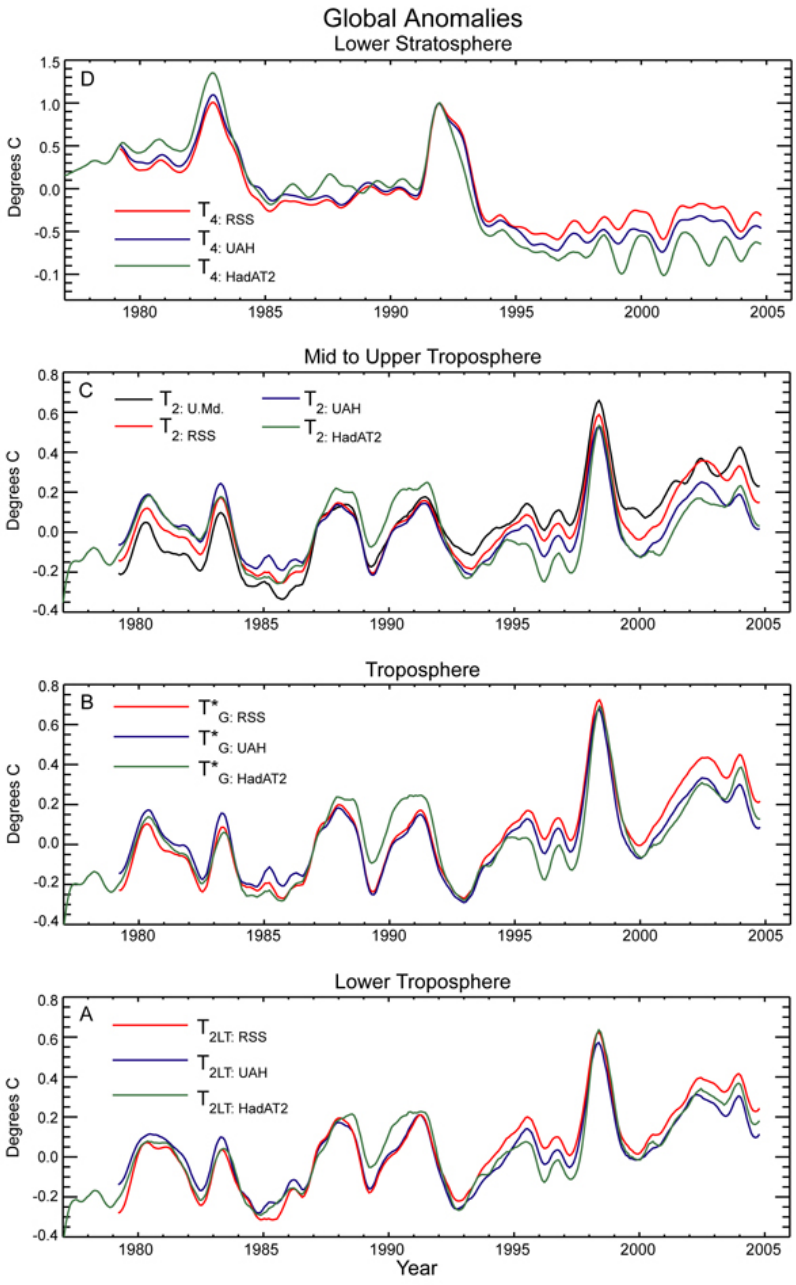

Figure 3.3a– Bottom: Time series of globally averaged lower tropospheric temperature (T2LT) as follows: UAH (blue) and RSS (red) satellite datasets, and HadAT2 (green) radiosonde data. All time series are 7-month running averages (used as a smoother) of original monthly data, which were expressed as a departure (ºC) from the 1979-97 average.

Figure 3.3b– Third: Time series of globally averaged middle tropospheric temperature (T*G) as follows: UAH (blue) and RSS (red) satellite datasets, and HadAT2 (green) radiosonde data. All time series are 7-month running averages (used as a smoother) of original monthly data, which were expressed as a departure (ºC) from the 1979-97 average.

Figure 3.3c – Second: Time series of globally averaged upper middle tropospheric temperature (T2) as follows: UAH) (blue), RSS (red), and U.Md. (black) satellite datasets, and HadAT2 (green) radiosonde data. All time series are 7-month running averages (used as a smoother) of original monthly data, which were expressed as a departure (ºC) from the 1979-97 average.

Figure 3.3d – Top: Time series of globally averaged lower stratospheric temperature (T4) as follows: UAH (blue) and RSS (red) satellite datasets, and HadAT2 (green) radiosonde data. All time series are 7-month running averages (used as a smoother) of original monthly data, which were expressed as a departure (ºC) from the 1979-97 average.

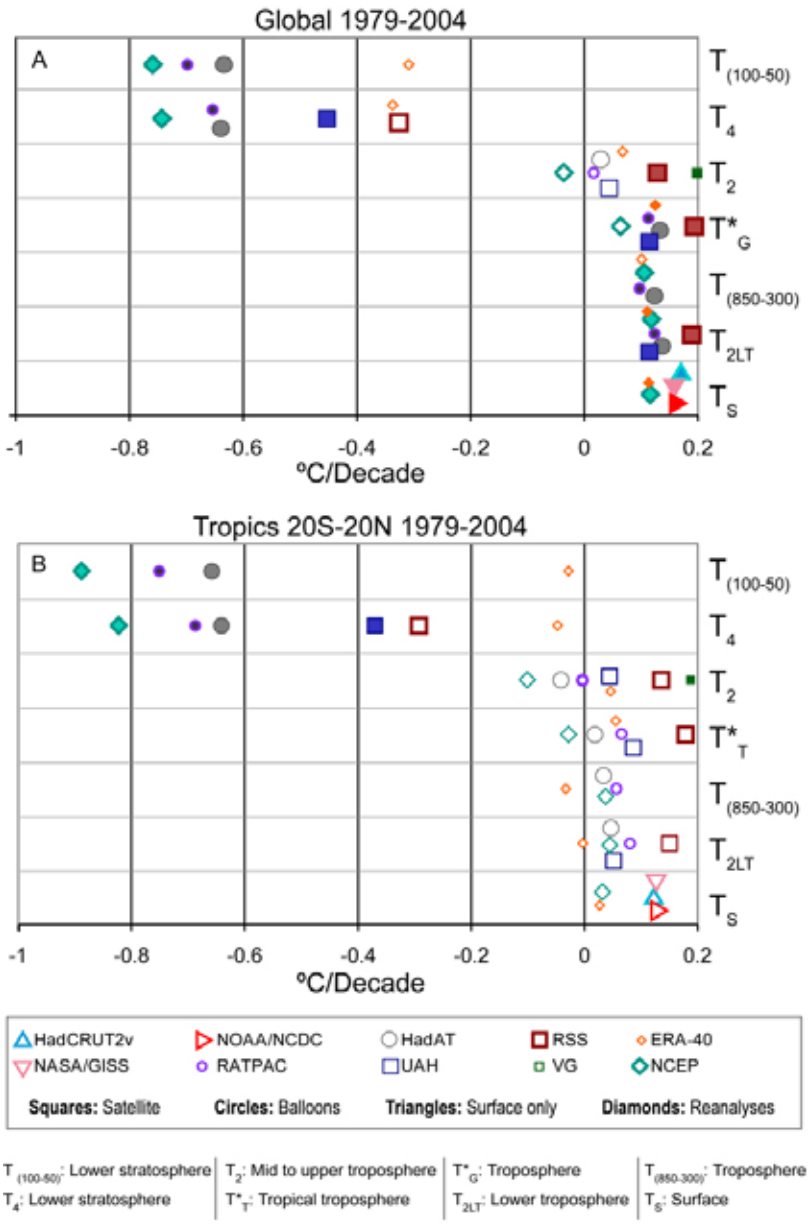

Figure 3.4a (top) – Global temperature trends (ºC/decade) for 1979-2004 from Table 3.3 plotted as symbols. See figure legend for definition of symbols. Filled symbols denote trends estimated to be statistically significantly different from zero (at the 5% level). A Student's t-test, using the lag-1 autocorrelation to account for the non-independence of residual values about the trend line, was used to assess significance (see Appendix for discussion of confidence intervals and significance testing).

Figure 3.4b (bottom) – Tropical (20oN-20oS) temperature trends (ºC/decade) for 1979-2004 from Table 3.4 plotted as symbols. See figure legend for definition of symbols. Filled symbols denote trends estimated to be statistically significantly different from zero (at the 5% level). A Student's t-test, using the lag-1 autocorrelation to account for the non-independence of residual values about the trend line, was used to assess significance (see Appendix for discussion of confidence intervals and significance testing).

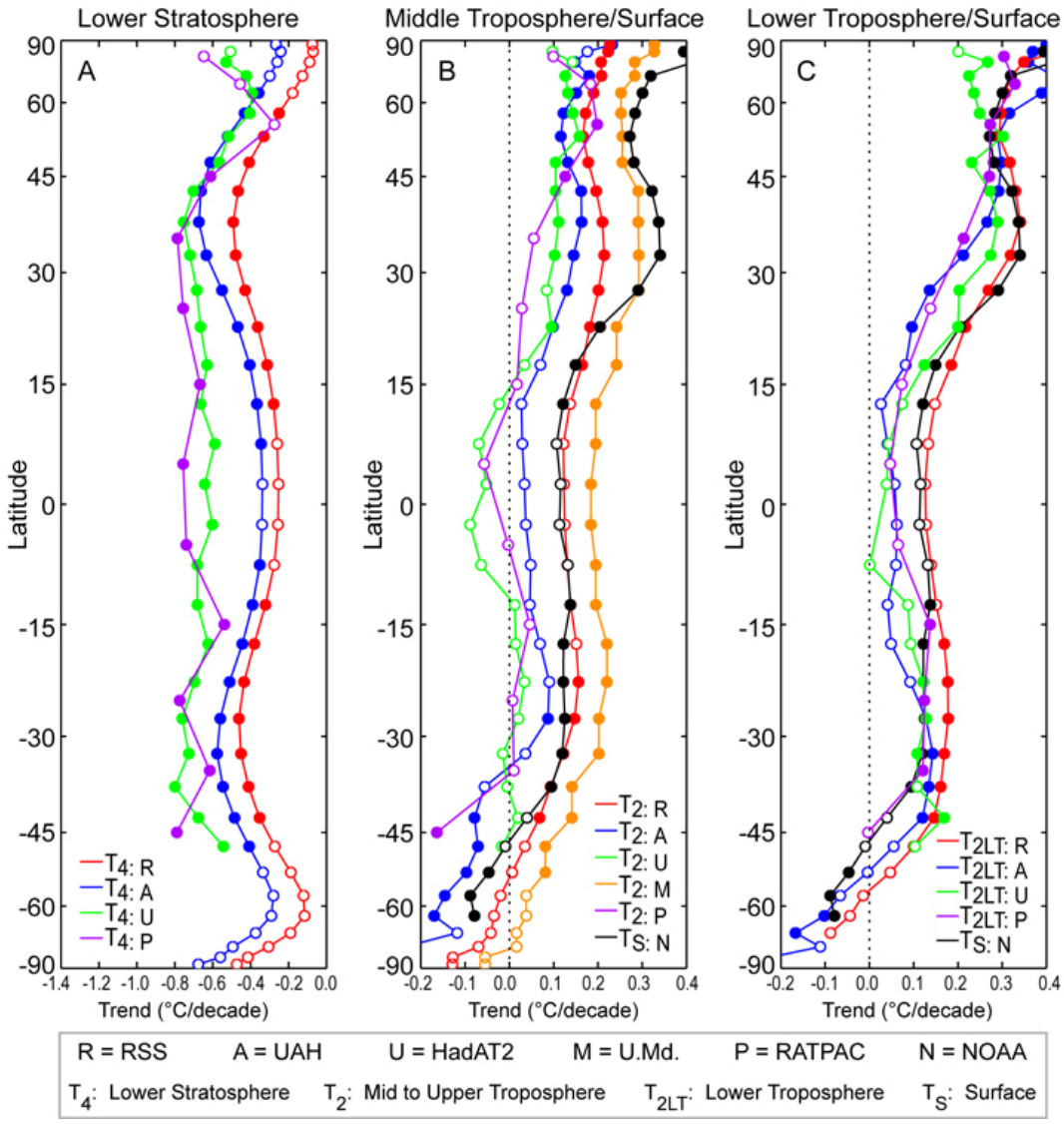

Figure 3.5 -- Temperature trends for 1979-2004 (ºC/decade) by latitude.

Left: stratospheric temperature (T_4) based on RSS (red) and UAH (blue) satellite datasets, and RATPAC (violet) and HadAT2 (green) radiosonde datasets.

Middle: mid-tropospheric temperature (T_2) based on U.Md. (orange), RSS (red) and UAH (blue) satellite datasets, and RATPAC (violet) and HadAT2 (green) radiosonde datasets; and surface temperature (T_S) from NOAA data (black).

Right: surface temperature (T_S) from NOAA data (black) and lower tropospheric temperature (T_{2LT}) from RSS (red) and UAH satellite data (blue), and from RATPAC (violet) and HadAT2 (green) radiosonde data. Filled circles denote trends estimated to be statistically significantly different from zero (at the 5% level). A Student's t-test, using the lag-1 autocorrelation to account for the non-independence of residual values about the trend line, was used to assess significance (see Appendix for discussion of confidence intervals and significance testing).

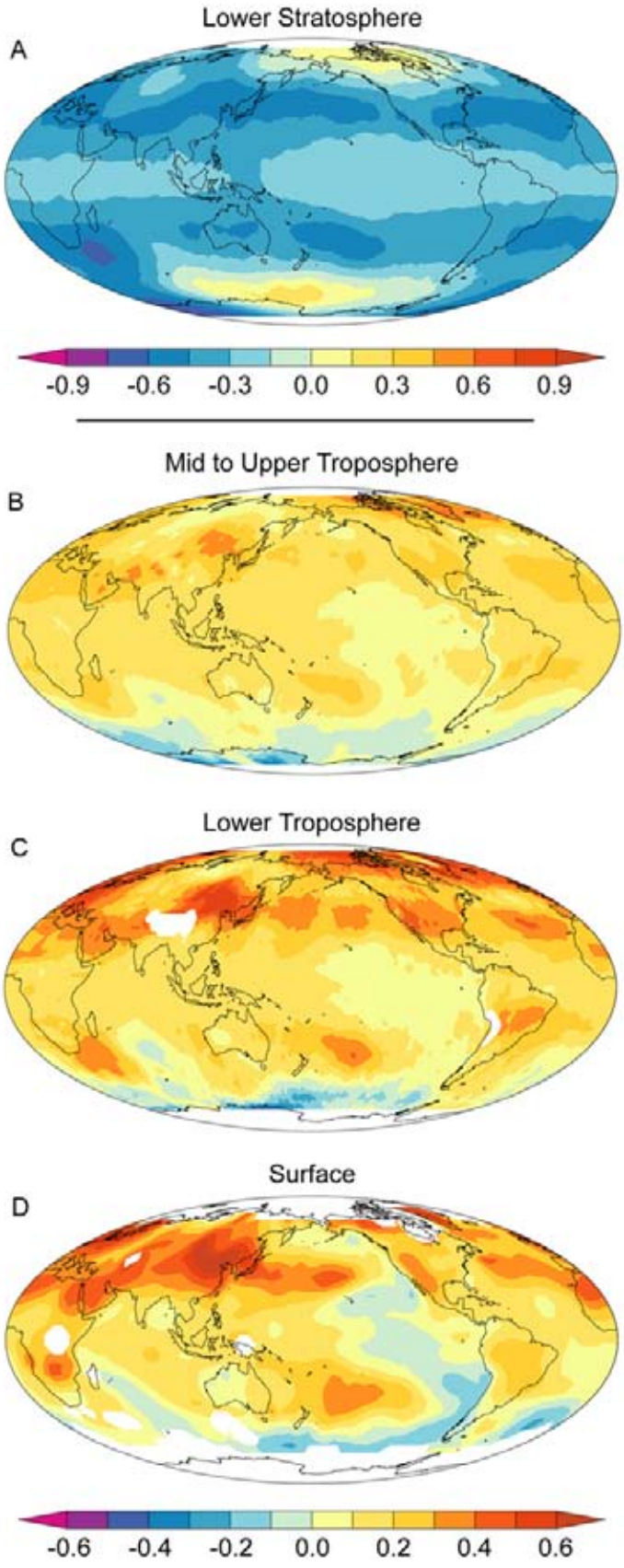

Figure 3.6 – Temperature trends for 1979-2004 (°C /decade).

Bottom (d): NOAA surface temperature (T_{S-N}).

Third (c): RSS lower tropospheric temperature (T_{2LT}-R).

Second (b): RSS upper middle tropospheric temperature (T_2-R).

Top (a): RSS lower stratospheric temperature (T_4-R).

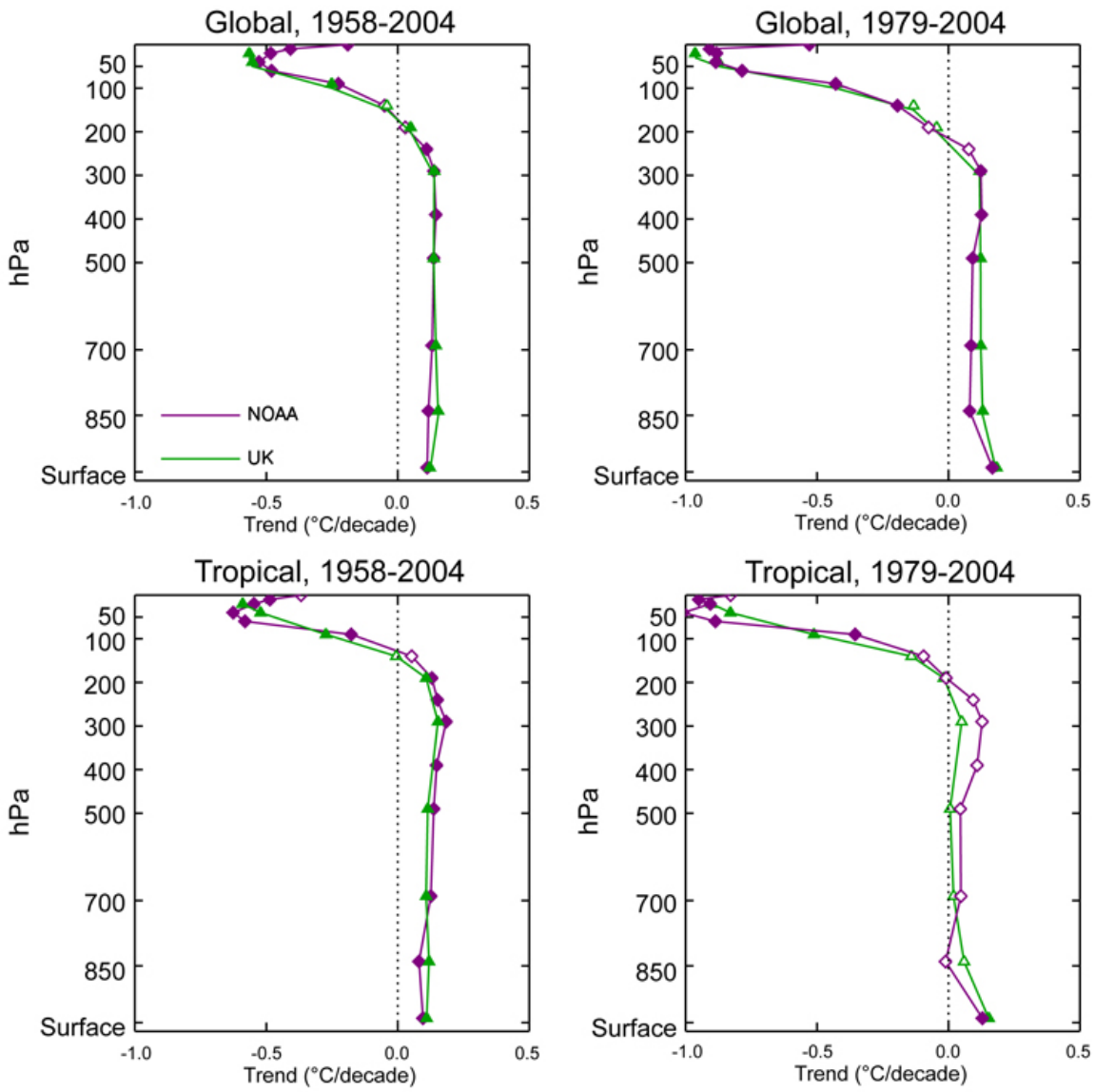

Figure 3.7 -- Vertical profiles of temperature trend (ºC/decade) as a function of altitude (i.e., pressure in hPa) computed from the RATPAC (violet) and HadAT2 (green) radiosonde datasets. Trends (which are given in Table 3.5) have been computed for 1958-2004 (left) and 1979-2004 (right) based on temperature that has been averaged over the globe (top) or the tropics, 20ºN-20ºS (bottom). Surface data for the HadAT2 product is taken from HadCRUT2v since the HadAT2 dataset does not include values at the surface; the surface values have been averaged so as to match their observing locations with those for the radiosonde data. By contrast, the surface temperatures from the RATPAC product are those from the RATPAC dataset, which are surface station values reported with the radiosonde data. Note that these differ from the NOAA surface dataset values (ER-GHCN-ICOADS) as indicated in Table 3.1. Filled symbols denote trends estimated to be statistically significantly different from zero (at the 5% level). A Student's t-test, using the lag-1 autocorrelation to account for the non-independence of residual values about the trend line, was used to assess significance (see Appendix for discussion of confidence intervals and significance testing).

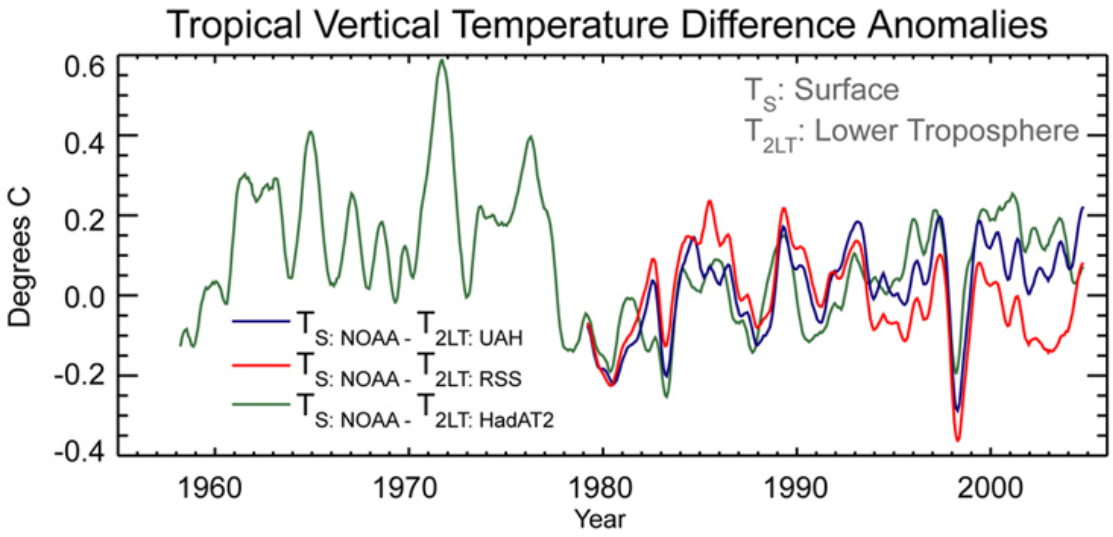

Figure 3.8 - Time series of vertical temperature difference (surface minus lower troposphere) for the tropics (20°N-20°S). NOAA surface temperatures (T_S-N) are used in each case to compute differences with lower tropospheric temperature (T_{2LT}) from three different groups: HadAT2 radiosonde (green), RSS satellite (red), and UAH satellite (blue). All time series are 7-month running averages (used as a smoother) of original monthly data, which were expressed as a departure (ºC) from the 1979-97 average.

CHAPTER 4

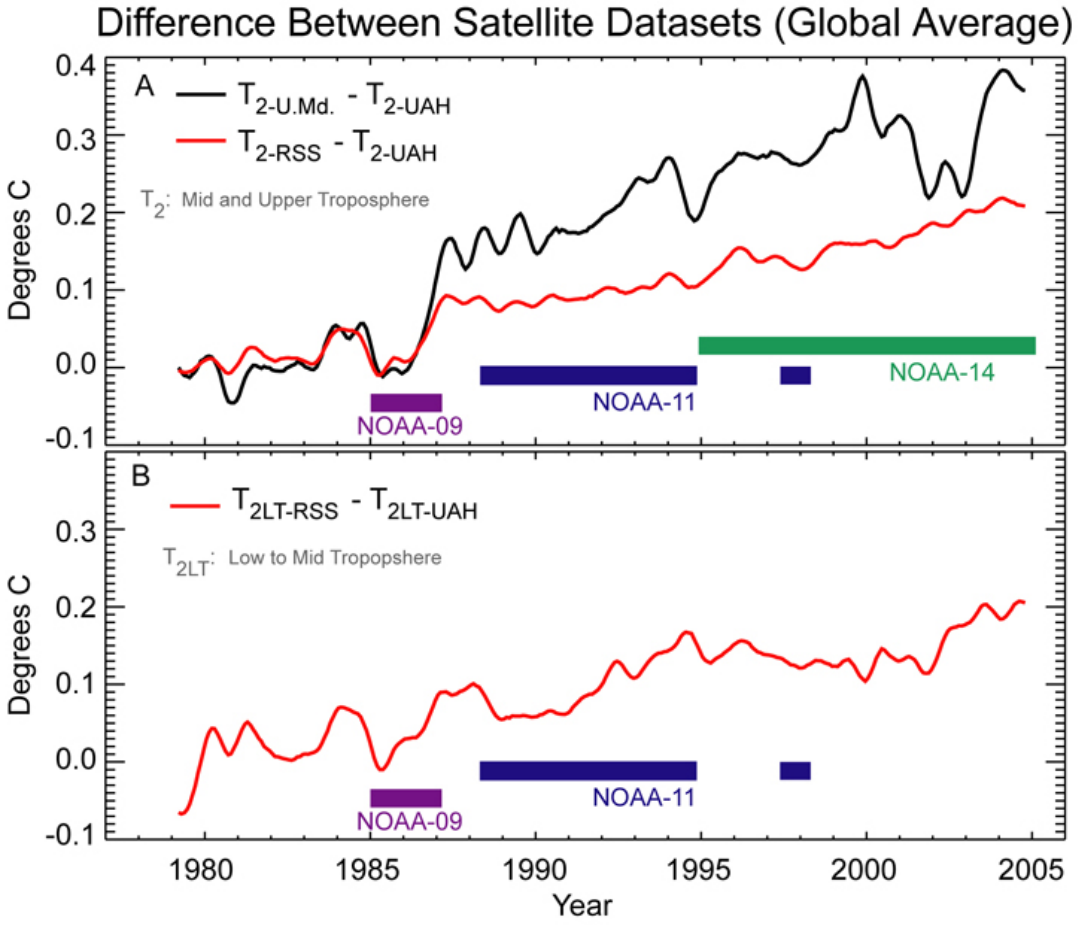

Figure 4.1 **(a)** Time series of the difference between global averages of satellite-derived T_2 datasets. Both the RSS and UMD datasets show a step-like feature relative to the UAH dataset during the lifetime of NOAA-09. The difference between the RSS and the UAH datasets shows a slow drift during the NOAA-11 and NOAA-14 lifetimes. Both these satellites drifted more than 4 hours in observations time. **(b)** Time series difference between global averages of satellite derived T_{2LT} datasets. A slow drift is apparent during the lifetime of NOAA-11, but the analysis during the NOAA-14 lifetime is complicated because the T_{2LT}-RSS dataset does not include data from the AMSU instruments on NOAA-15 and NOAA-16, while the T_{2LT}-UAH dataset does. All time series have been smoothed using a Gaussian filter with width = 7 months.

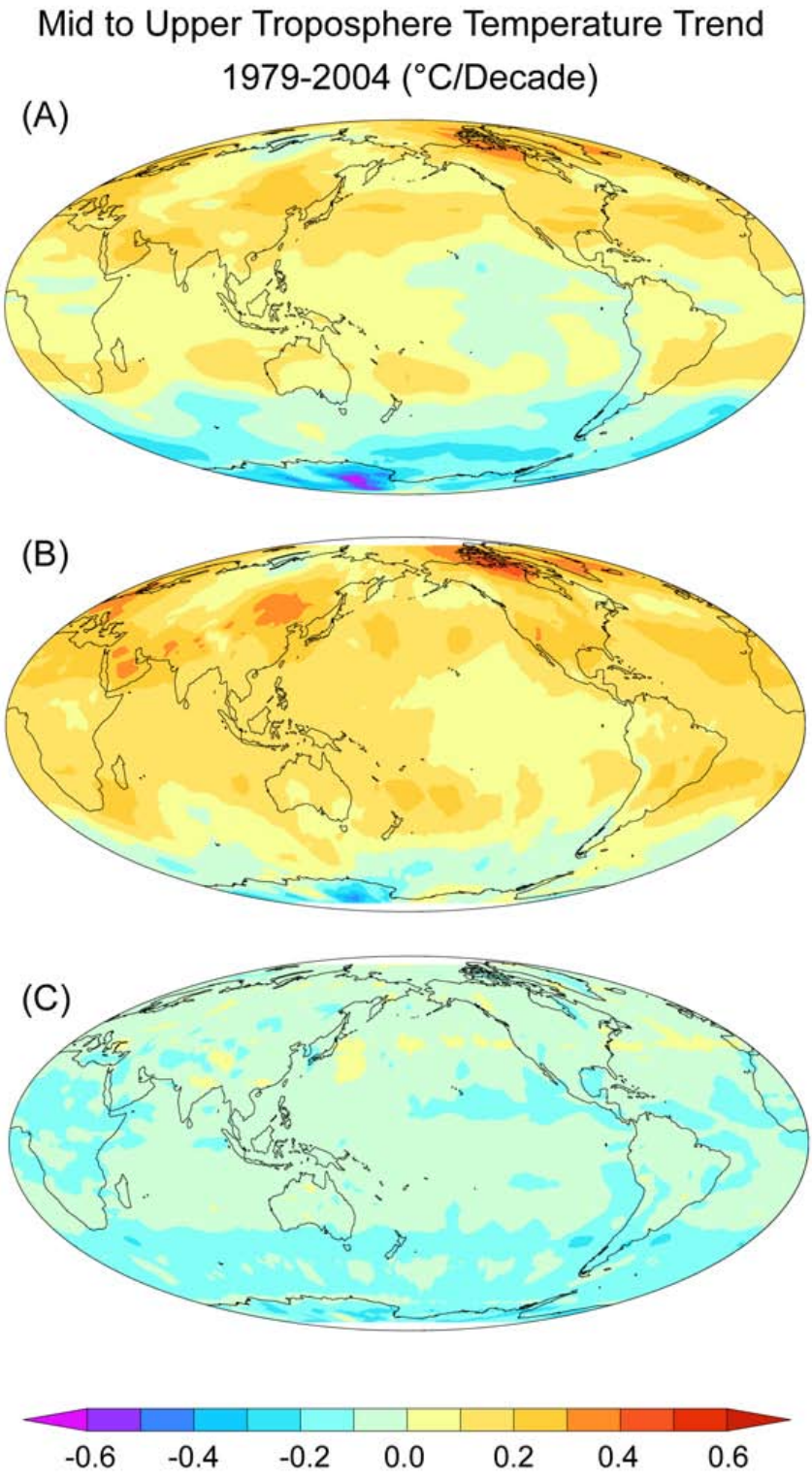

Figure 4.2 Global maps of trends from 1979-2004 for **(a)** T_2-UAH and **(b)** T_2-RSS. Except for an overall difference between the two results, the spatial patterns are very similar. A map of the difference T_2-UAH – T_2-RSS between trends for the two products shown in **(c)** reveals more subtle differences in the trend.

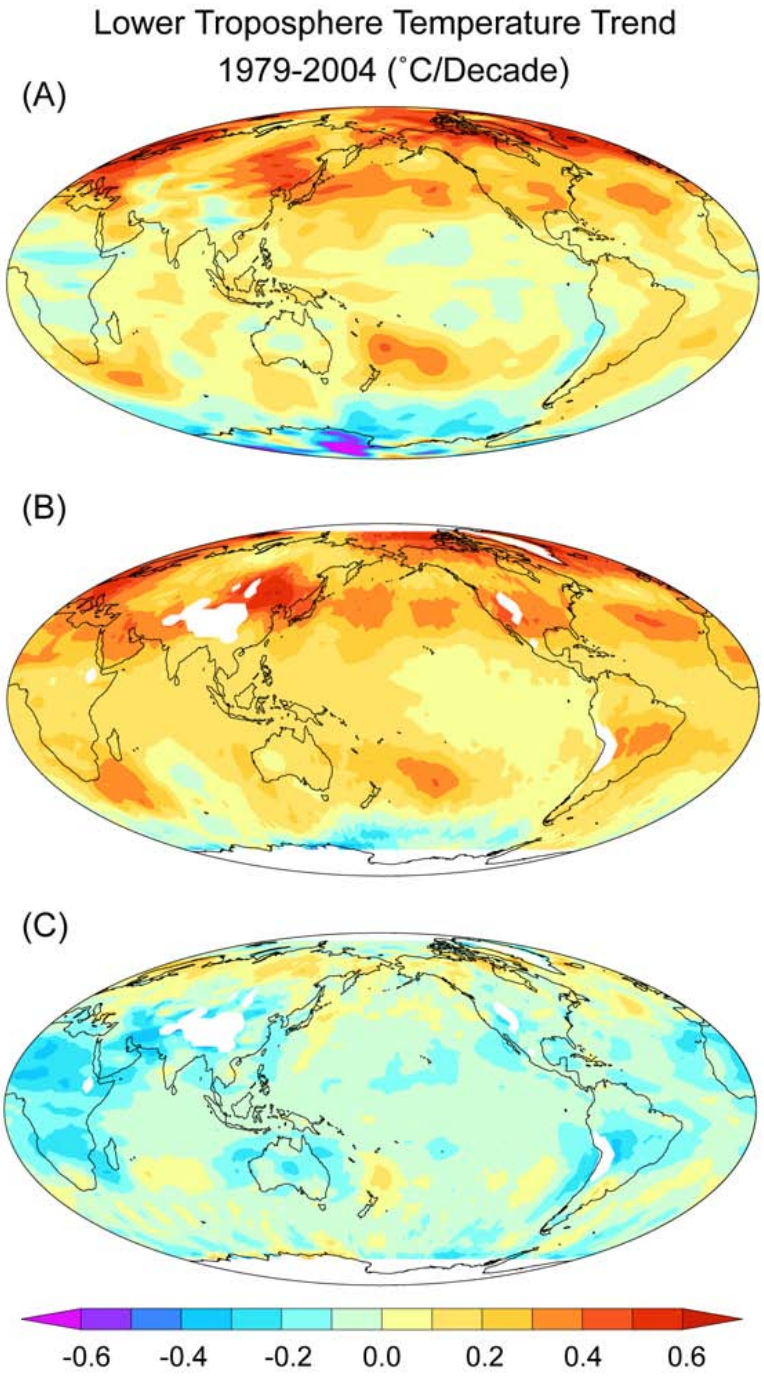

Figure 4.3 Global maps of trends from 1979-2004 for **(a)** T_{2LT}-UAH and **(b)** T_{2LT}-RSS. Except for an overall difference between the two results, the spatial patterns are similar. A map of the difference T_{2LT}-UAH – T_{2LT}-RSS between trends for the two products shown in **(c)** shows that the largest differences are over tropical and subtropical land areas. Data from land areas with elevation higher than 2000m are excluded from the T_{2LT}-RSS dataset and shown in white.

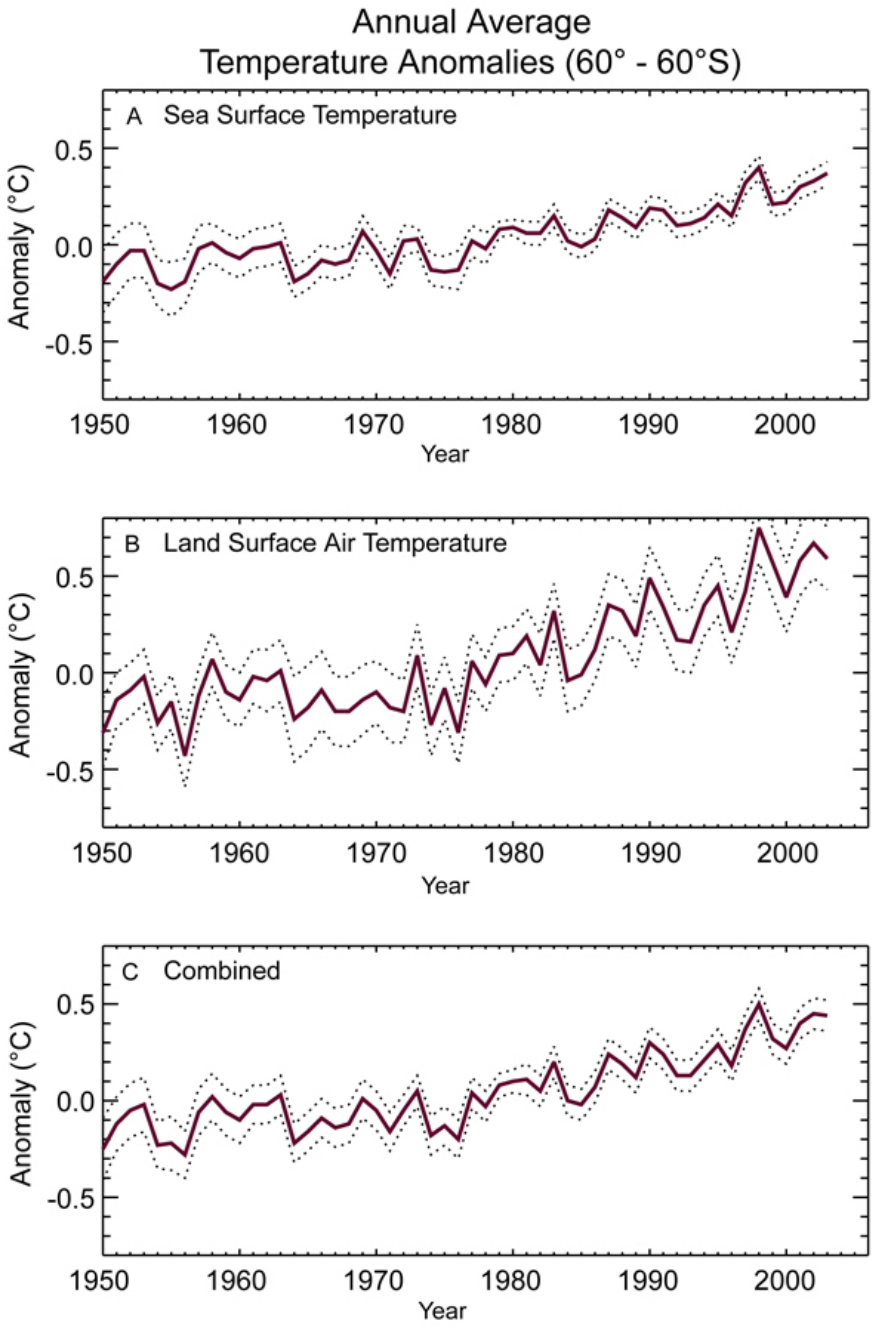

Figure 4.4. SST, Land Surface Air Temperature, and the Combined Temperature Data Record anomaly averaged annually and between 60ºS and 60ºN (purple), with its estimated 95% confidence intervals (dashed). Data are from the NOAA GHCN-ERSST dataset (Smith and Reynolds 2005).

CHAPTER 5

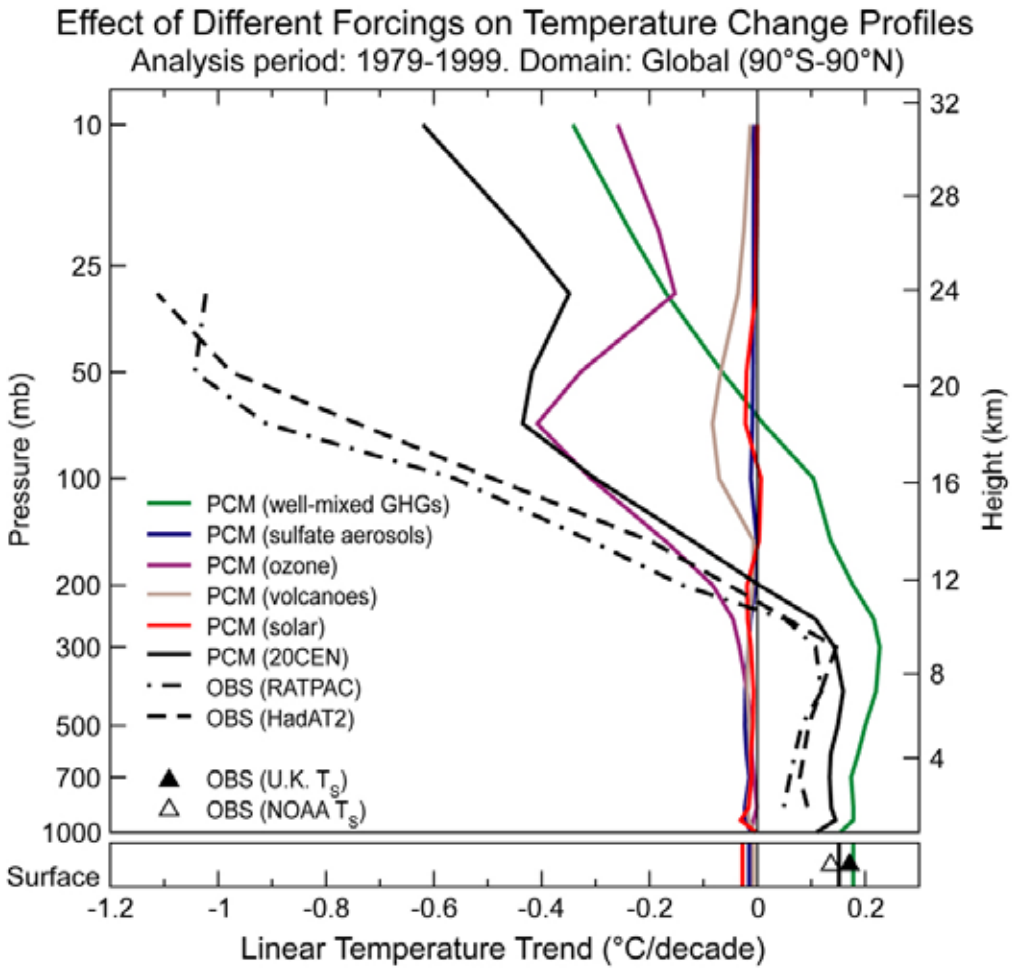

Figure 5.1: Vertical profiles of global-mean atmospheric temperature change over 1979 to 1999. Surface temperature changes are also shown. Results are from two different radiosonde data sets (HadAT2 and RATPAC; see Chapter 3) and from single forcing and combined forcing experiments performed with the Parallel Climate Model (PCM; Washington et al., 2000). PCM results for each forcing experiment are averages over four different realizations of that experiment. All trends were calculated with monthly mean anomaly data.

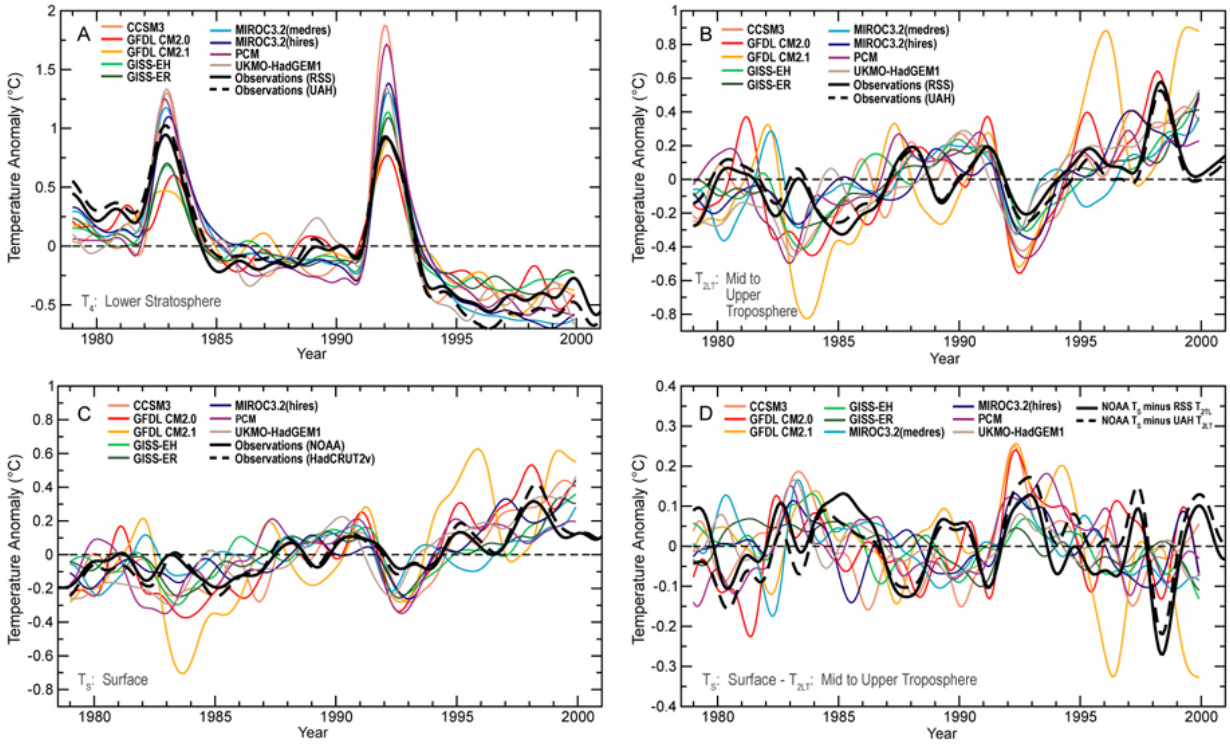

Figure 5.2A: Modeled and observed changes in global-mean monthly-mean lower stratospheric temperature (T4). A simple weighting function approach (Box 2.2) was used to calculate a "synthetic" T4 (equivalent to the MSU T4 monitored by satellites) from model temperature data. Synthetic T4 results are from "20CEN" experiments performed with nine different models (see Table 5.1). These models were chosen because they satisfy certain minimum requirements in terms of the forcings applied in the 20CEN run: all nine were driven by changes in well-mixed GHGs, sulfate aerosol direct effects, tropospheric and stratospheric ozone, volcanic aerosols, and solar irradiance (in addition to other forcings; see Table 5.2). Observed satellite-based estimates of T4 changes were obtained from both RSS and UAH (see Chapter 3). All T4 changes are expressed as departures from a 1979 to 1999 reference period average, and were smoothed with the same filter. To make it easier to compare the variability of T4 in models with different ensemble sizes (see Table 5.1), only the first 20CEN realization is plotted from each model. This also facilitates comparisons of modeled and observed variability.

Figure 5.2B: As for Figure 5.2A, but for time series of global-mean, monthly-mean lower tropospheric temperature anomalies (T2LT).

Figure 5.2C: As for Figure 5.2A, but for time series of global-mean, monthly-mean surface temperature anomalies (TS).

Figure 5.2D: As for Figure 5.2A, but for time series of global-mean, monthly-mean temperature differences between the surface and T2LT.

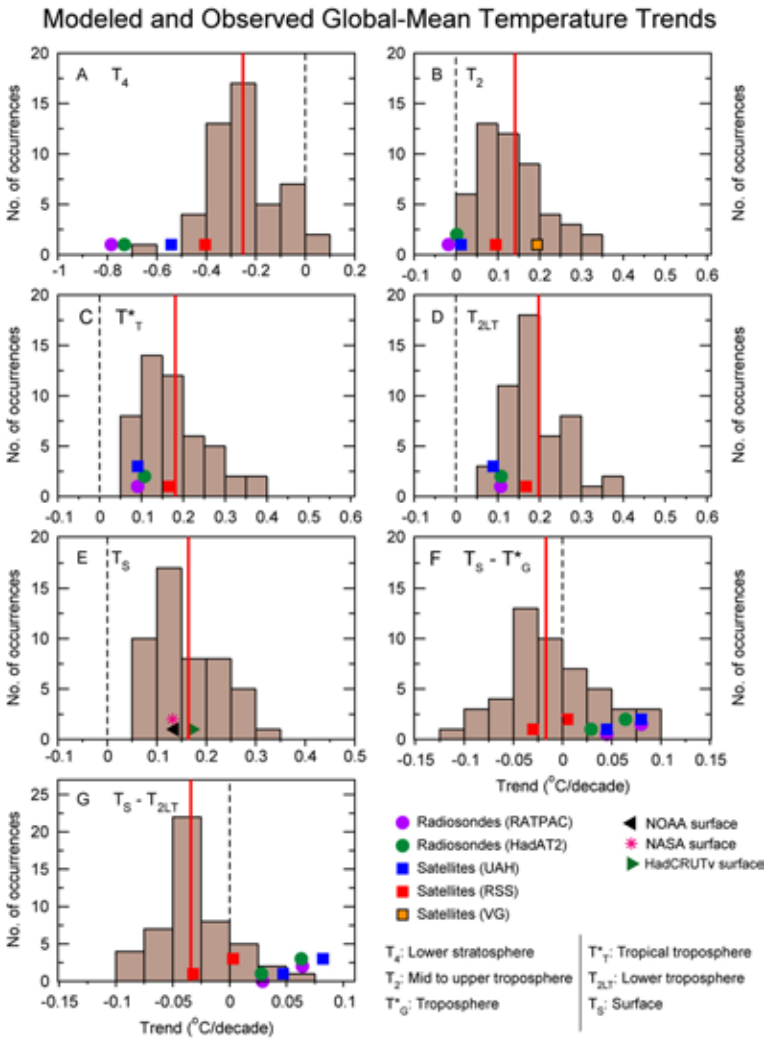

Figure 5.3: Modeled and observed trends in time series of global-mean T4 (panel A), T2 (panel B), T*G (panel C), T2LT (panel D), TS (panel E), TS minus T*G (panel F), and TS minus T2LT. All trends were calculated using monthly-mean anomaly data. The analysis period is 1979 to 1999. Model results are displayed in the form of histograms. Each histogram is based on results from 49 individual realizations of the 20CEN experiment, performed with 19 different models (Table 5.1). The applied forcings are listed in Table 5.2. The vertical red line in each panel is the mean of the model trends, calculated with a sample size of n = 19 (see Table 5.4A). Observed trends are estimated from two radiosonde and three satellite datasets (T2), two radiosonde and two satellite datasets (T4, T*G and T2LT), and three different surface datasets (TS) (see Chapter 3). The bottom "rows" of the observed difference trends in panels F and G were calculated with NOAA TS data. The top "rows" of observed results in F and G were computed with HadCRUT2v TS data. The vertical offsetting of observed results in these panels (and also in panels B-E) is purely for the purpose of simplifying the visual display – observed trends bear no relation to the y-axis scale. To simplify the display, the Figure does not show the statistical uncertainties arising from the fitting of linear trends to noisy data. GISS TS trends (not shown) are very close to those estimated with NOAA TS data (see Chapter 3).

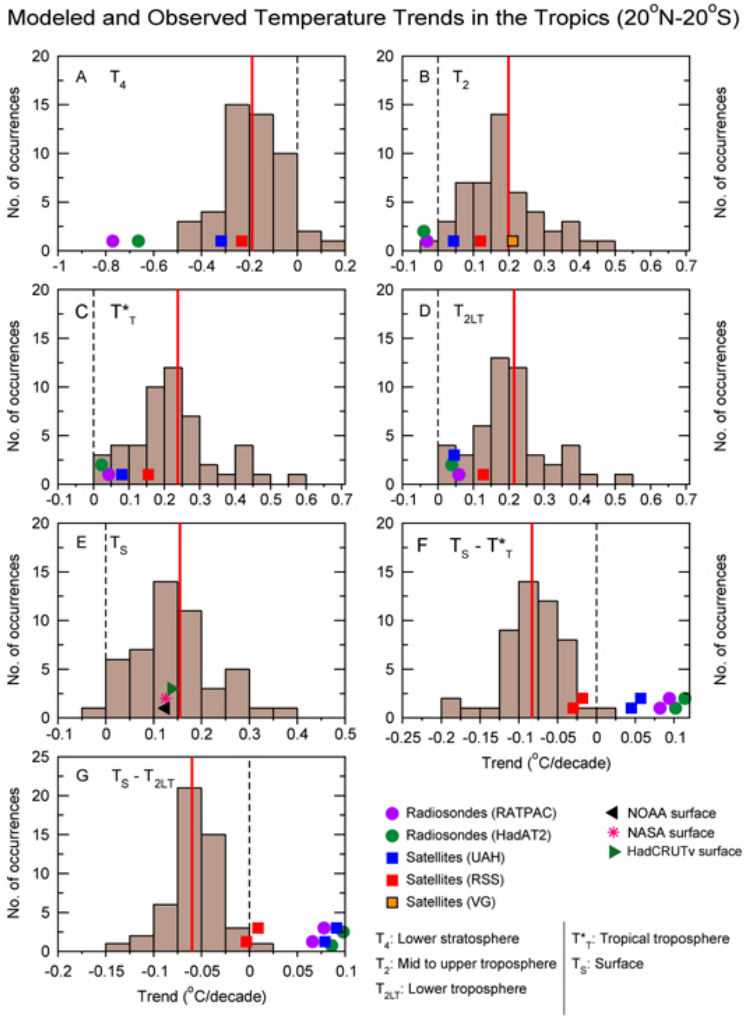

Figure 5.4: As for Figure 5.3, but for trends in the tropics (20°N-20°S).

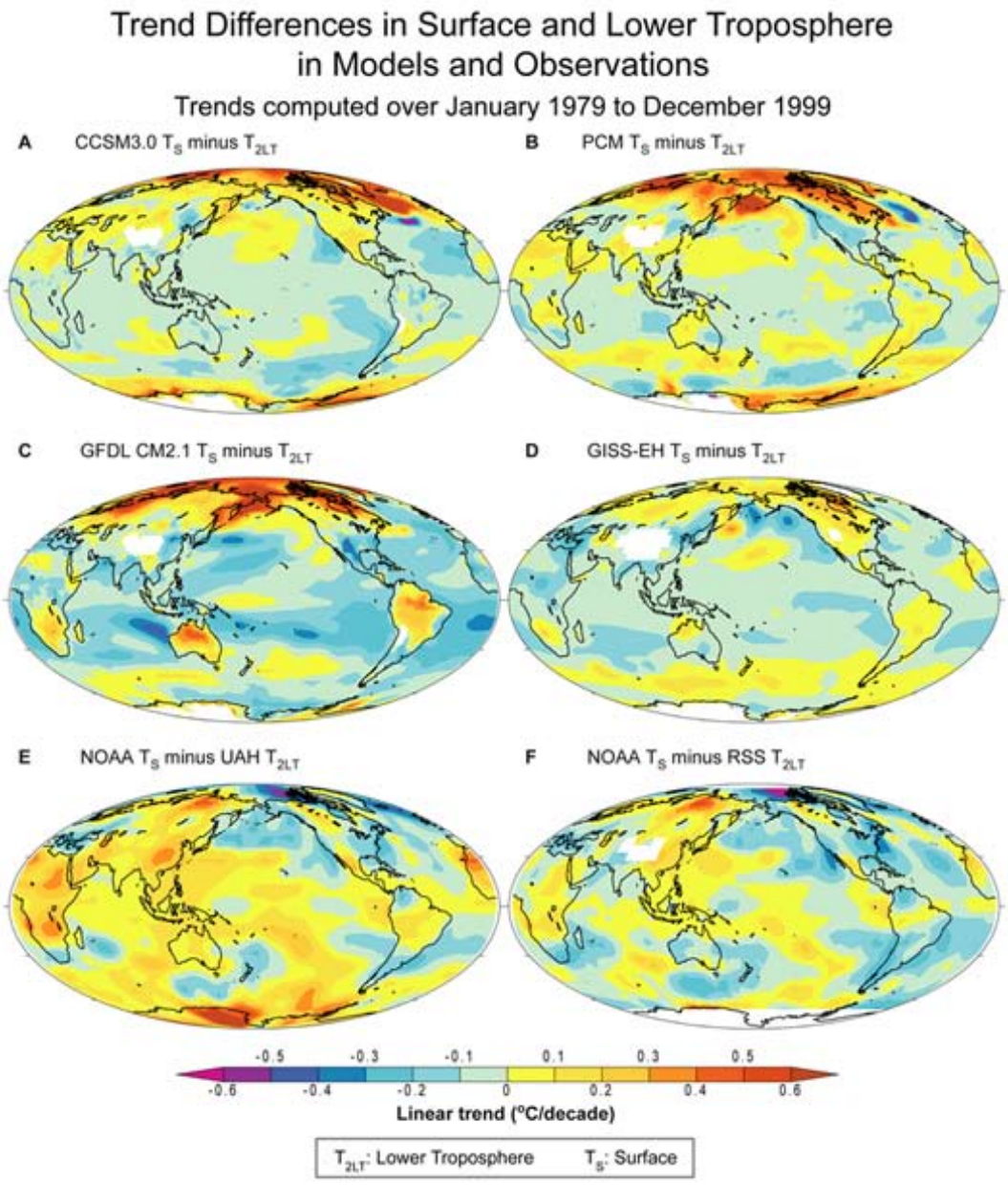

Figure 5.5: Modeled and observed maps of the differences between trends in TS and T2LT. All trends in TS and T2LT were calculated over the 252-month period from January 1979 to December 1999. Model results are ensemble means from 20CEN experiments performed with CCSM3.0 **(panel A)**, PCM **(panel B)**, GFDL CM2.1 **(panel C)**, and GISS-EH **(panel D)**. Observed results rely on NOAA TS trends and on two different satellite estimates of trends in T2LT, obtained from UAH **(panel E)** and RSS **(panel F).** White denotes high elevation areas where it is not meaningful to calculate synthetic T2LT **(panels A-D)**. Note that RSS mask T2LT values in such regions, while UAH do not **(c.f. panels F, E).**

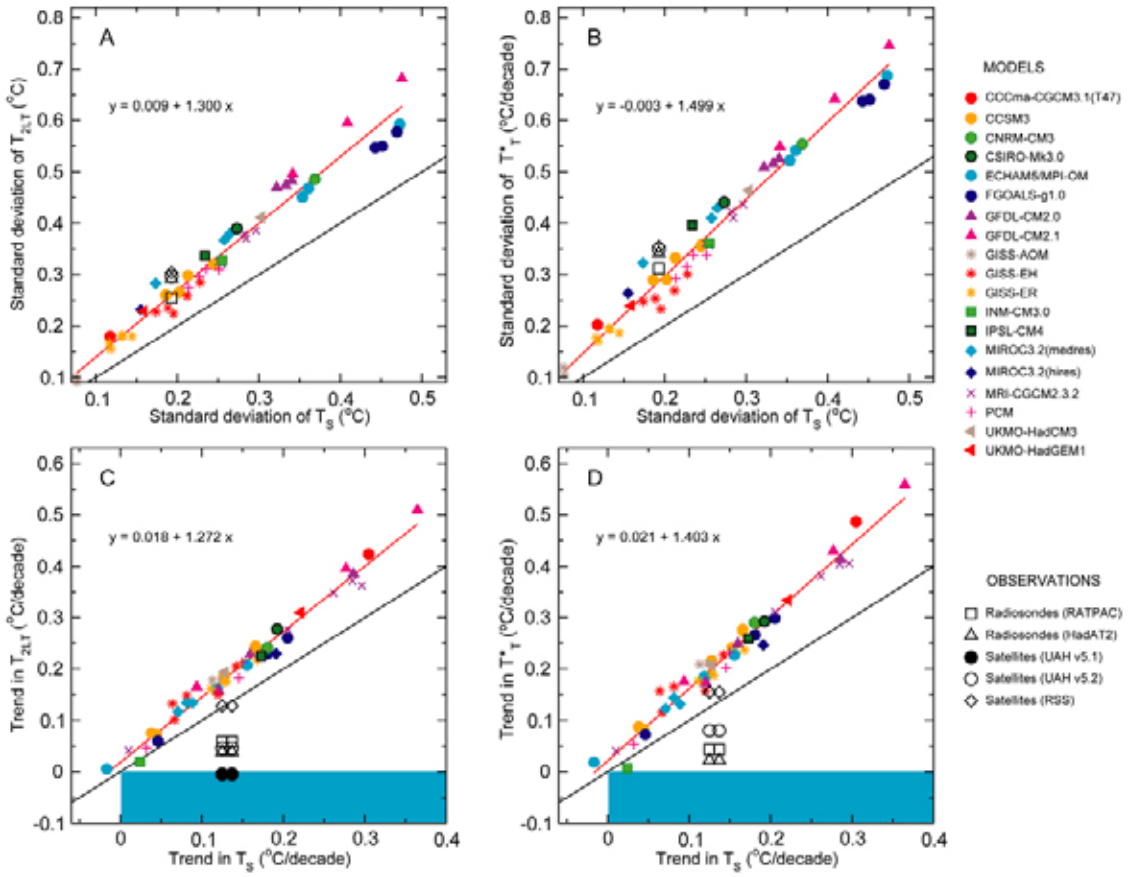

Figure 5.6: Scatter plots showing the relationships between tropical temperature changes at Earth's surface and in two different layers of the troposphere. All results rely on temperature data that have been spatially-averaged over the deep tropics (20°N-20°S). Model data are from 49 realizations of 20CEN runs performed with 19 different models (Table 5.1). Observational results were taken from four different upper-air datasets (two from satellites, and two from radiosondes) and two different surface temperature datasets (see Chapter 3). The two upper panels provide information on the month-to-month variability in TS and T2LT **(panel A)** and in TS and T*T **(panel B)**. The two bottom panels consider temperature changes on multi-decadal timescales, and show the trends (over 1979 to 1999) in TS and T2LT **(panel C)** and in TS and T*T **(panel D)**. The red line in each panel is the regression line through the model points. Its slope provides information on the amplification of surface temperature variability and trends in the free troposphere. The black line in each panel is given for reference purposes, and has a slope of 1. Values above (below) the black lines indicate tropospheric amplification (damping) of surface temperature changes. There are two columns of observational results in C and D. These are based on the NOAA and HadCRUT2v TS (0.12 and 0.14°C/decade, respectively). Note that panel C show results from published and recently-revised versions of the UAH T2LT data (versions 5.1 and 5.2). Since the standard deviations calculated from NOAA and HadCRUT2v monthly TS anomalies are very similar, observed results in A and B use NOAA standard deviations only. The blue shading in the bottom two panels defines the region of simultaneous surface warming and tropospheric cooling.

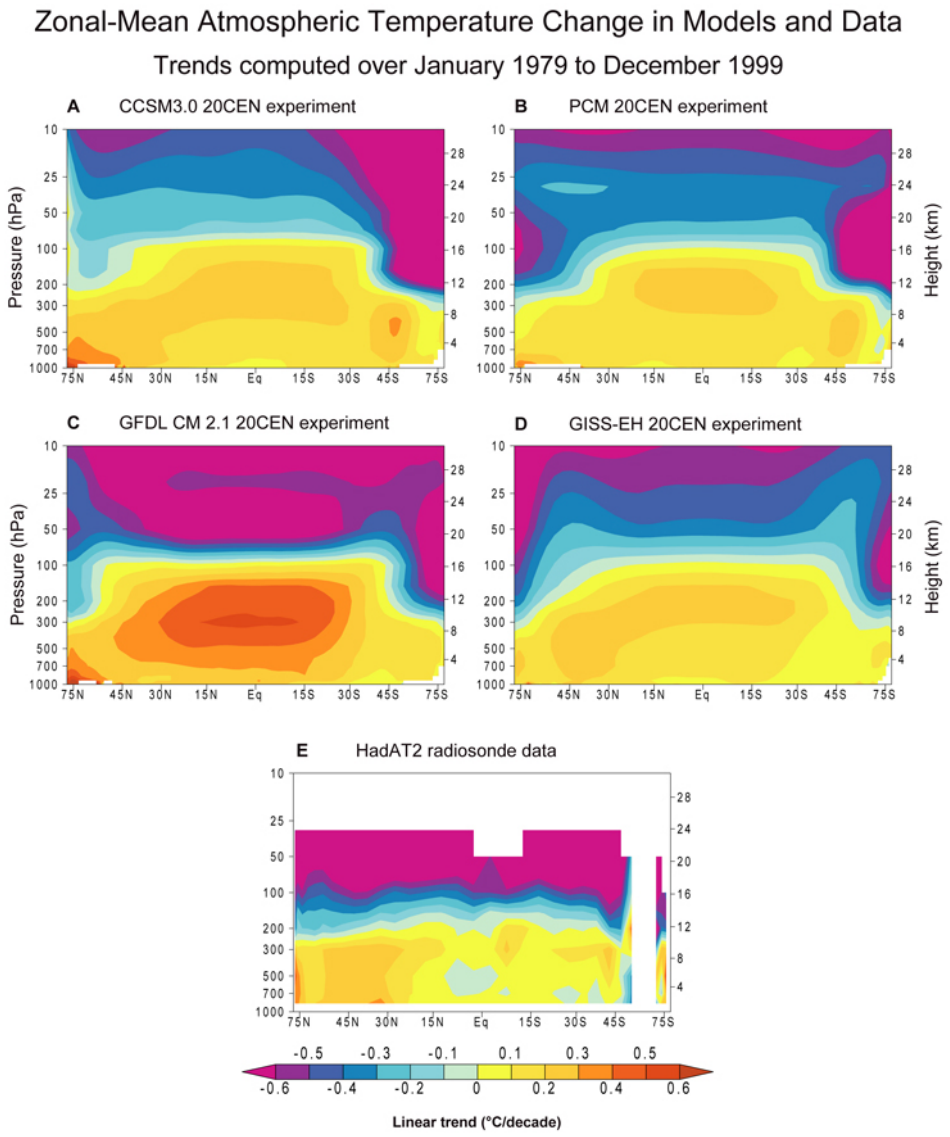

Figure 5.7: Zonal-mean patterns of atmospheric temperature change in "20CEN" experiments performed with four different climate models and in observational radiosonde data. Model results are for CCSM3.0 **(panel A),** PCM **(panel B),** GFDL CM 2.1 **(panel C),** and GISS-EH **(panel D).** The model experiments are ensemble means. There are differences between the sets of climate forcings that the four models used in their 20CEN runs (Table 5.3). Observed changes **(panel E)** were estimated with HadAT2 radiosonde data (Thorne et al., 2005, and Chapter 3). The HadAT2 temperature data do not extend above 30 hPa, and have inadequate coverage at high latitudes in the Southern Hemisphere. All temperature changes were calculated from monthly-mean data and are expressed as linear trends (in °C/decade) over 1979 to 1999.

CHAPTER 6
(Does not contain figures)

APPENDIX: STATISTICAL ISSUES REGARDING TREND

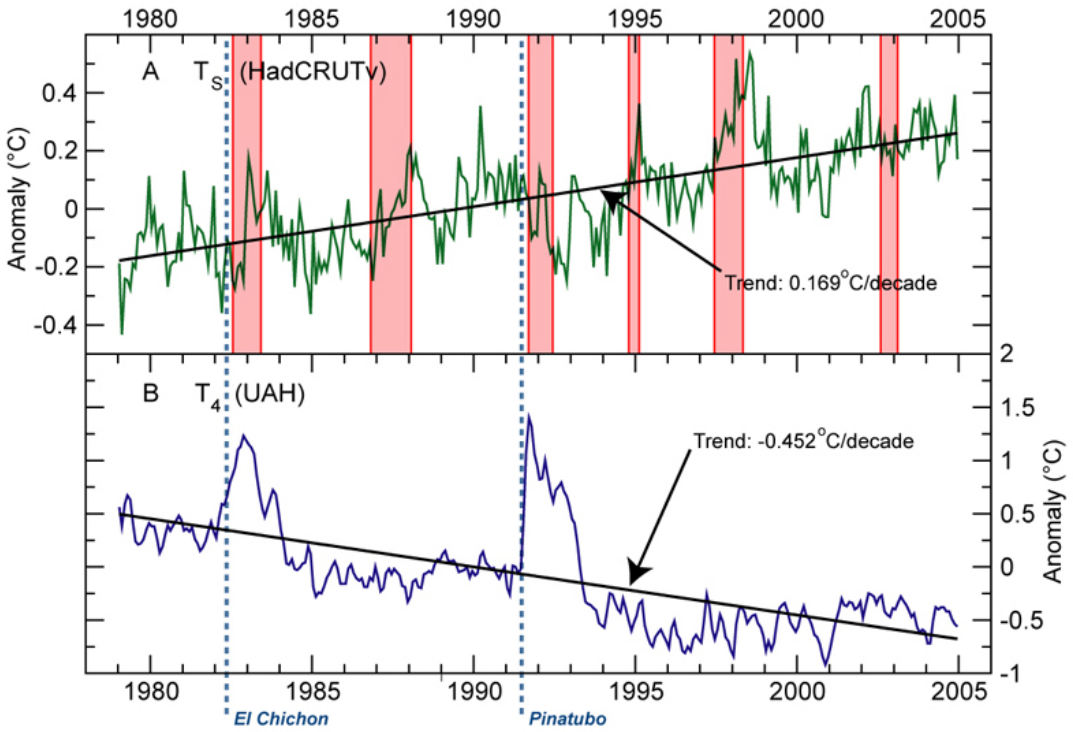

Appendix Figure 1: Examples of temperature time series with best-fit (least squares) linear trends: A, global-mean surface temperature from the UKMO Hadley Centre/Climatic Research Unit data set (HadCRUTv); and B, MSU channel 4 data (T_4) for the lower stratosphere from the University of Alabama at Huntsville (UAH). Note the much larger temperature scale on the lower panel. Temperature changes are expressed as anomalies relative to the 1979 to 1999 mean (252 months). Dates for the eruptions of El Chichon and Pinatubo are shown by vertical lines. El Niños are shown by the shaded areas. These were defined by low-pass filtering of the Southern Oscillation Index (SOI) time series with an 11-month, 9-term Gaussian filter and using a threshold index value of –0.7 to define an event.

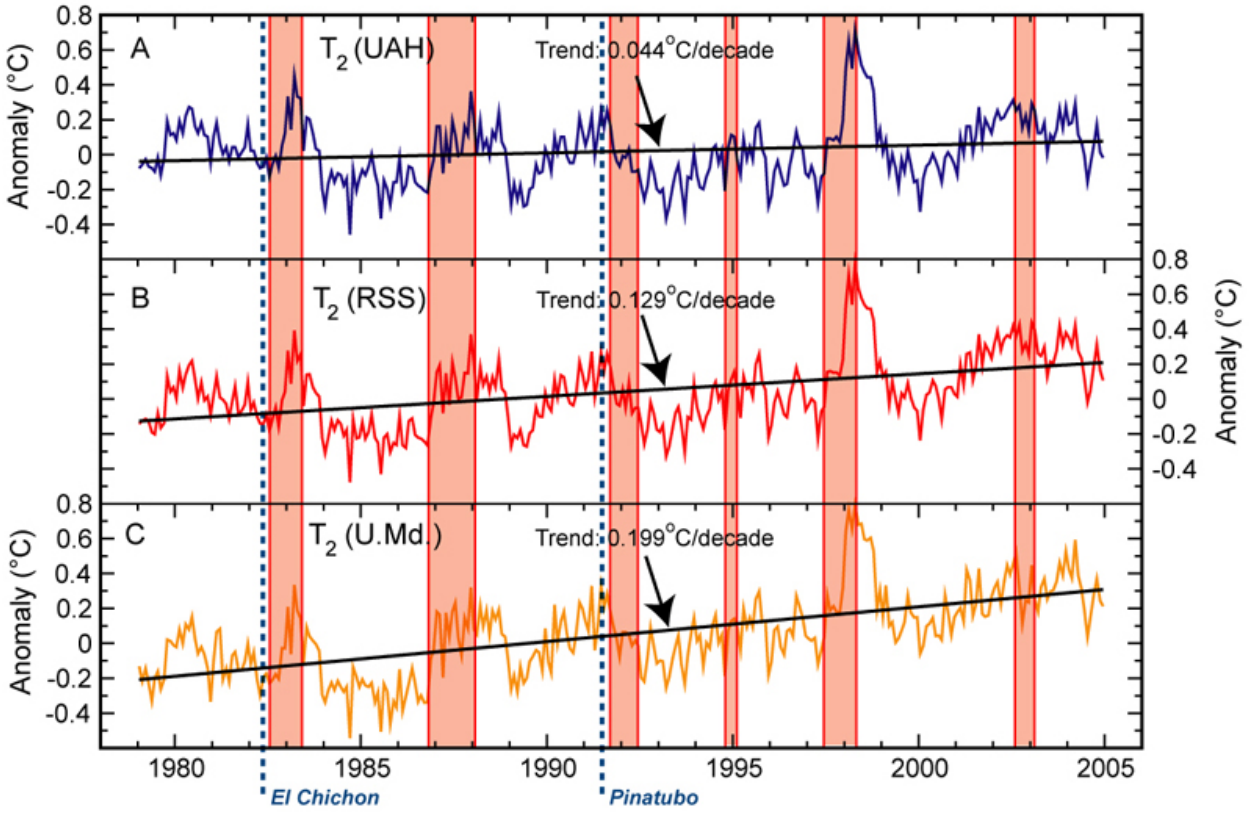

Appendix Figure 2: Three estimates of temperature changes for MSU channel 2 (T_2), expressed as anomalies relative to the 1979 to 1999 mean. Data are from: A, the University of Alabama at Huntsville (UAH); B, Remote Sensing Systems (RSS); and C, the University of Maryland (U.Md.) The estimates employ the same 'raw' satellite data, but make different choices for the adjustments required to merge the various satellite records and to correct for instrument biases. The statistical uncertainty is virtually the same for all three series. Differences between the series give some idea of the magnitude of structural uncertainties. Volcano eruption and El Niño information are as in Figure 1.

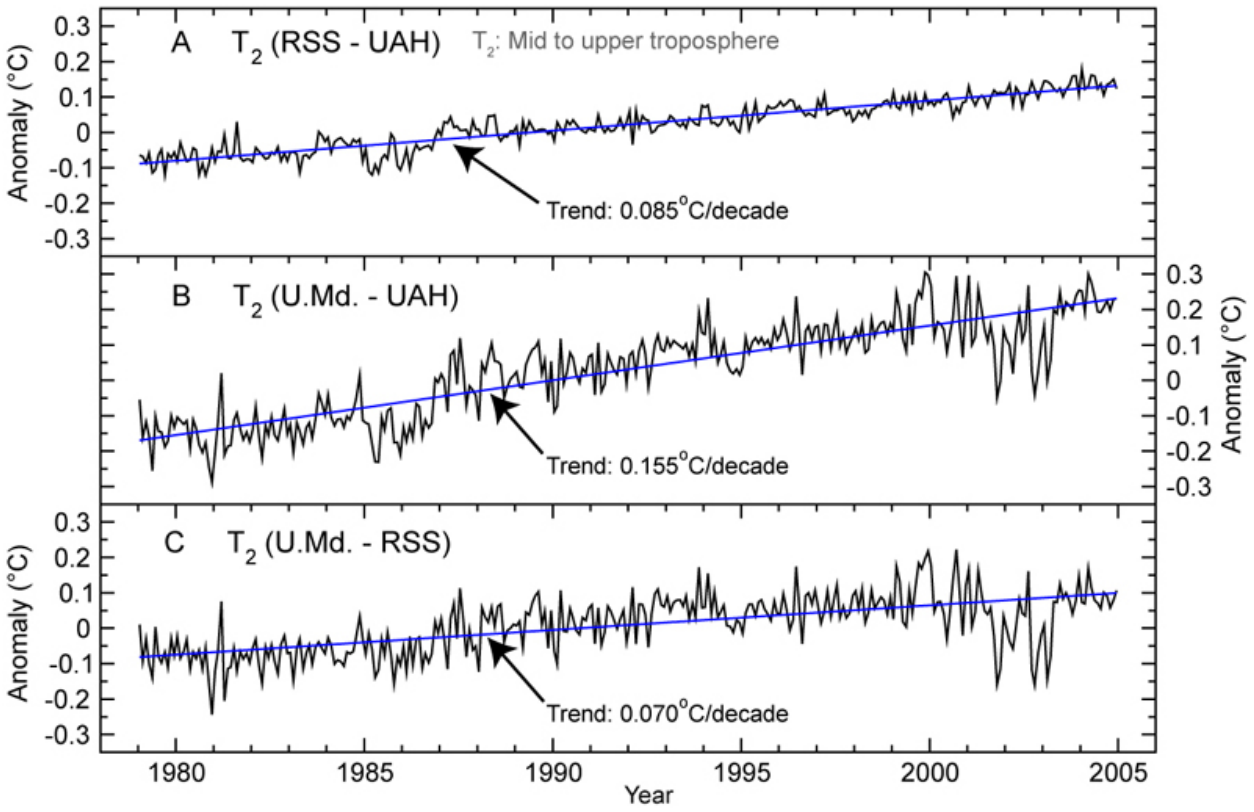

Appendix Figure 3: Difference series for the MSU T_2 series shown in Figure 2. Variability about the trend line is least for the UAH minus RSS series indicating closer correspondence between these two series than between U.Md. and either UAH or RSS.

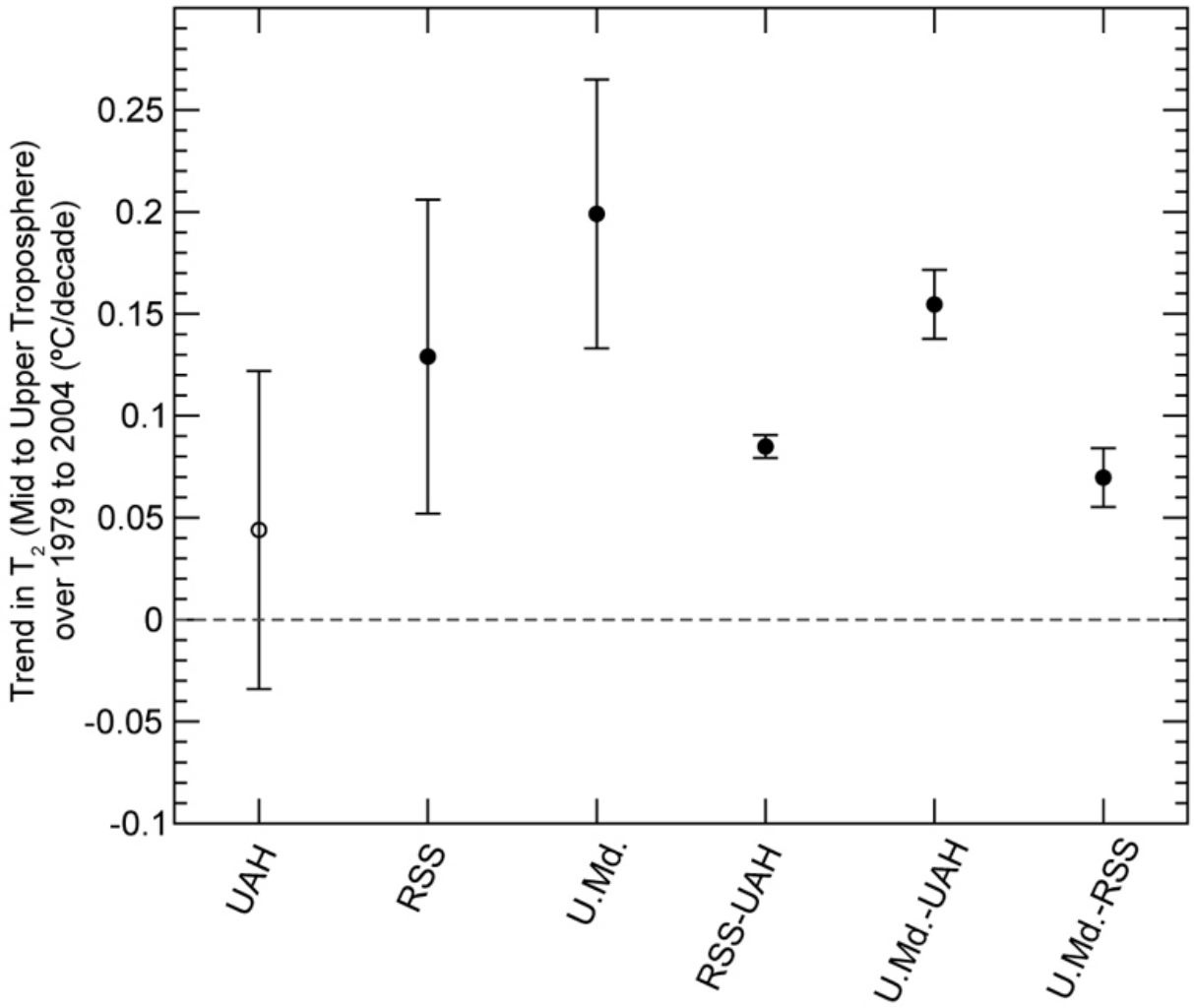

Appendix Figure 4: 90% confidence intervals for the three MSU T_2 series shown in Figure 2, and for the three difference series shown in Figure 3.

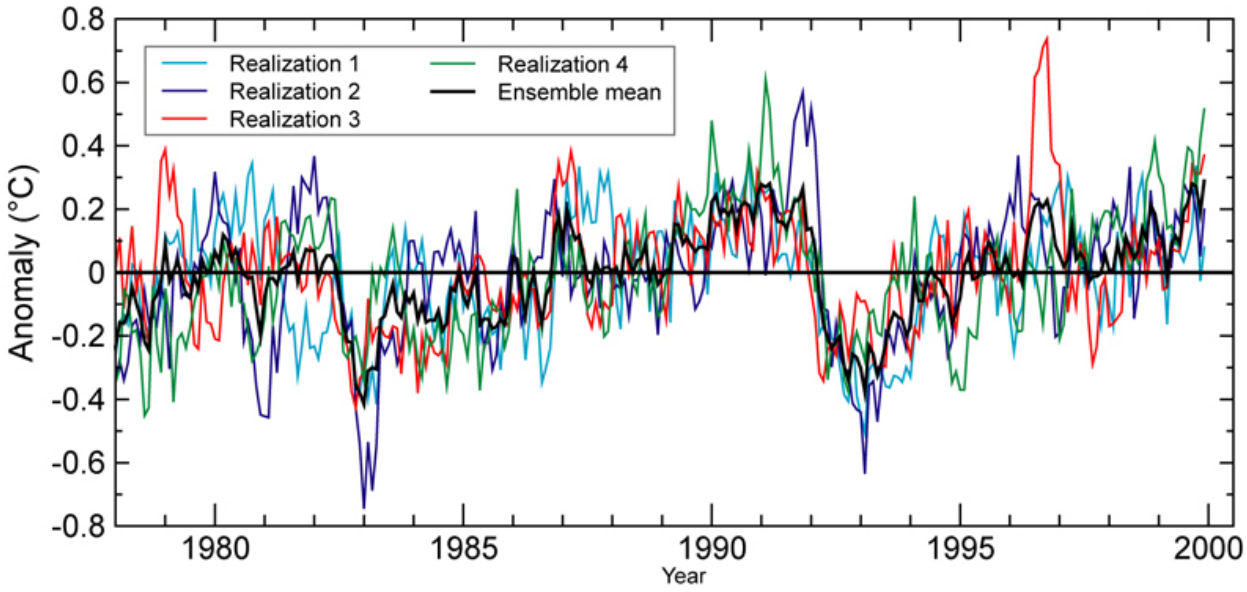

Appendix Figure 5: Four separate realizations and their ensemble average for a simulation using realistic 20th Century forcing (both natural and anthropogenic) carried out with the xxx AOGCM.

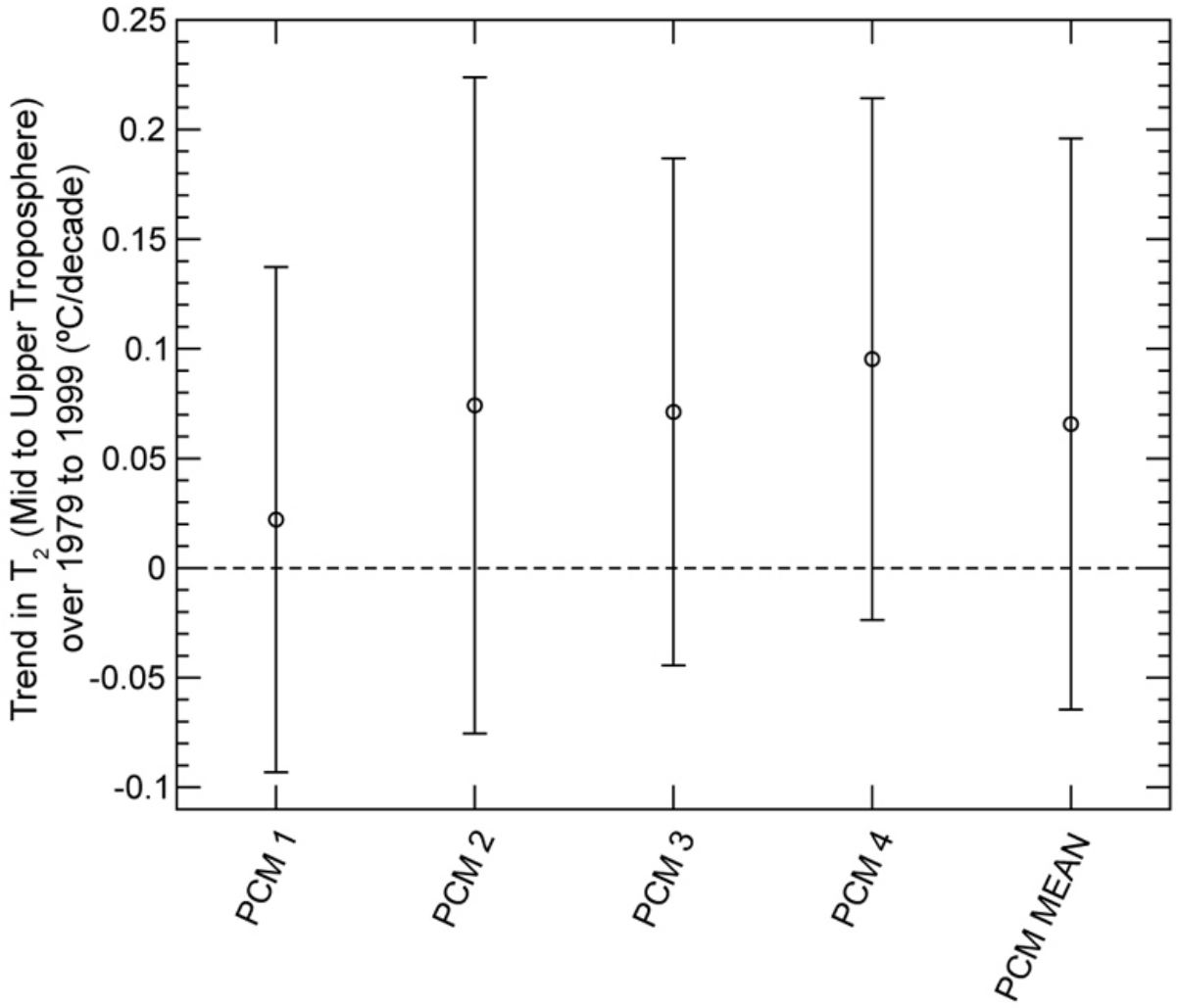

Appendix Figure 6: 90% confidence intervals for individual model realizations of MSU T_2 temperature changes, compared with the 90% confidence interval for the ensemble (n=4) average.